



**HAL**  
open science

## Advantages and limitations of different methods to determine the optimum formulation in surfactant-oil-water systems: A review

R. Marquez, Jesus Ontiveros, N. Barrios, L. Tolosa, G. Palazzo, Véronique Rataj, J. L. Salager

### ► To cite this version:

R. Marquez, Jesus Ontiveros, N. Barrios, L. Tolosa, G. Palazzo, et al.. Advantages and limitations of different methods to determine the optimum formulation in surfactant-oil-water systems: A review. *Journal of Surfactants and Detergents*, 2023, *Journal of Surfactants and Detergents*, -, 10.1002/jsde.12703 . hal-04269578

**HAL Id: hal-04269578**

**<https://hal.univ-lille.fr/hal-04269578v1>**

Submitted on 3 Nov 2023

**HAL** is a multi-disciplinary open access archive for the deposit and dissemination of scientific research documents, whether they are published or not. The documents may come from teaching and research institutions in France or abroad, or from public or private research centers.

L'archive ouverte pluridisciplinaire **HAL**, est destinée au dépôt et à la diffusion de documents scientifiques de niveau recherche, publiés ou non, émanant des établissements d'enseignement et de recherche français ou étrangers, des laboratoires publics ou privés.



Distributed under a Creative Commons Attribution 4.0 International License

## Force Tensiometer DCAT

The most versatile laboratory device for analysing detergents and surfactants

- surface & interfacial tension of liquids
- dynamic contact angles
- critical micelle concentration (CMC)
- density of liquids and solids
- adhesive force
- surface pressure
- interfacial rheology of monolayers



**dataphysics**  
Understanding Interfaces

DataPhysics Instruments GmbH  
Raiffeisenstraße 34 • 70794 Filderstadt, Germany  
phone +49 (0)711 770556-0 • fax +49 (0)711 770556-99  
sales@dataphysics-instruments.com  
www.dataphysics-instruments.com

Learn more >

# Advantages and limitations of different methods to determine the optimum formulation in surfactant–oil–water systems: A review

Ronald Marquez<sup>1,2</sup>  | Jesús F. Ontiveros<sup>3</sup>  | Nelson Barrios<sup>2,4</sup>  |  
 Laura Tolosa<sup>5</sup>  | Gerardo Palazzo<sup>6</sup>  | Véronique Nardello-Rataj<sup>3</sup>  |  
 Jean Louis Salager<sup>7</sup> 

<sup>1</sup>ESPCI Paris, PSL University, Paris, France

<sup>2</sup>Department of Forest Biomaterials, North Carolina State University, Raleigh, North Carolina, USA

<sup>3</sup>Univ. Lille, CNRS, Centrale Lille, Univ. Artois, UMR 8181, UCCS, Unité de Catalyse et Chimie du Solide, Lille, France

<sup>4</sup>Laboratory of Petroleum, Hydrocarbons and Derivatives, University of Carabobo, Valencia, Venezuela

<sup>5</sup>Polymers and Colloids Laboratory, School of Chemical Engineering, University of the Andes, Mérida, Venezuela

<sup>6</sup>Department of Chemistry, University of Bari, and CSGI (Center for Colloid and Surface Science), Bari, Italy

<sup>7</sup>FIRP Laboratory, School of Chemical Engineering, University of the Andes, Mérida, Venezuela

## Correspondence

Ronald Marquez, Department of Forest Biomaterials, North Carolina State University, Raleigh, North Carolina, USA.  
 Email: [rjmarque@ncsu.edu](mailto:rjmarque@ncsu.edu)

Jesús F. Ontiveros and Véronique Nardello-Rataj, Univ. Lille, CNRS, Centrale Lille, Univ. Artois, UMR 8181, UCCS, Unité de Catalyse et Chimie du Solide Lille, France.  
 Email: [jesus-fermin.ontiveros@centralelille.fr](mailto:jesus-fermin.ontiveros@centralelille.fr) and [veronique.rataj-nardello@univ-lille.fr](mailto:veronique.rataj-nardello@univ-lille.fr)

Jean Louis Salager, FIRP Laboratory, School of Chemical Engineering, University of the Andes, Mérida, Venezuela.  
 Email: [jl.salager@gmail.com](mailto:jl.salager@gmail.com)

## Abstract

The optimum formulation in a surfactant–oil–water (SOW) system is defined as the physicochemical situation at which the surfactant adsorbed at the interface exhibits exactly equal interactions for both oil and water. Identifying the optimum formulation of SOW systems is crucial in various industrial applications, ranging from pharmaceuticals to cosmetics and to petroleum issues like dehydration and enhanced oil recovery. Multiple techniques are available to identify the optimum formulation, often with its own advantages and limitations. In this comprehensive review, we provide an in-depth analysis of the systematic use of formulation scans to identify the optimum formulation in SOW systems. We critically assess different methods, including conventional ones, such as phase behavior observation, determination of the minimum interfacial tension from equilibrated systems, and the localization of the minimum emulsion stability using formulation scans. We also mention a new promising technique that can be applied in practice, such as oscillating spinning drop interfacial rheology (OSDIR) as well as others that allow an understanding of some structural features of the domains present in the surfactant-rich phase in SOW systems. Among these methods, dynamic light scattering (DLS), small angle scattering (SAXS and SANS), nuclear magnetic resonance (NMR), X-ray microcomputed tomography (Micro-CT), and differential scanning calorimeter (DSC), can be found in the literature. Finally, we discuss potentially unusual behaviors that can appear in complex systems, thus providing guidance on the selection of the most suitable method tailored to the specific application.

## KEYWORDS

dilational rheology, DLS, formulation scans, HLD, interfacial tension, NMR, optimum formulation, phase transition, SAXS, surfactant/oil/water systems

## INTRODUCTION

Surfactant–oil–water (SOW) systems are found in numerous applications such as food, pharmaceuticals,

personal care products, paints, cleaning and detergency, petroleum production, fuels, and wastewater treatment (Salager, 2002; Salager, Marquez, Bullon, & Forgiarini, 2022; Tadros, 2006). At low concentrations

This is an open access article under the terms of the [Creative Commons Attribution](https://creativecommons.org/licenses/by/4.0/) License, which permits use, distribution and reproduction in any medium, provided the original work is properly cited.

© 2023 The Authors. *Journal of Surfactants and Detergents* published by Wiley Periodicals LLC on behalf of AOCS.

of surfactant, SOW systems at equilibrium exhibit three distinct behaviors, as indicated by Winsor in its pioneering work, that is, Winsor I, Winsor II, and Winsor III phase behaviors (Bourrel & Schechter, 2010). In the Winsor III case, at the optimum formulation (nowadays described by the hydrophilic-lipophilic deviation, at  $HLD_N = 0$ ), the interaction between the surfactant, and the oil and water phases are exactly balanced, leading to the so-called bicontinuous microemulsion system, as explained by Scriven in 1976 (Bourrel & Schechter, 2010; Salager, Marquez, Bullon, & Forgiarini, 2022; Scriven, 1976; Winsor, 1954). Winsor initially described this phenomenon in the 1950s and 1960s (Winsor, 1968). Subsequently, the optimum formulation concept was introduced in the mid-1970s at the minimum in interfacial tension for enhanced oil recovery (EOR) with surfactant flooding techniques in the petroleum industry (Cayias et al., 1975; Reed & Healy, 1977). Salager et al. (Salager, 1977; Salager, Bourrel, et al., 1979) developed the multivariable equation, known today as the Hydrophilic-Lipophilic Deviation (HLD) (Salager, 1977; Salager, Morgan, et al., 1979). It is well established that the optimum formulation corresponds to a minimum in interfacial tension, which is described in the situation of  $HLD_N$  equal to zero (Forgiarini et al., 2021; Marquez, Meza, Alvarado, Johnny, et al., 2021; Salager et al., 2020; Salager, Marquez, Delgado-Linares, et al., 2022). Other system variables can also be used to identify the optimum formulation, such as the maximum of the solubilization parameter when a formulation scan is performed (Huh, 1979; Salager et al., 2020; Salager, Forgiarini, & Bullón, 2013).

In 1979, Salager, Wade, and Schechter first published the multivariable equation that described the physicochemical formulation situation for ionic surfactants (Salager, Morgan, et al., 1979). This was followed in 1980 by Bourrel, Salager, Wade, and Schechter's publication of the multivariable equation for nonionic surfactants (Bourrel et al., 1980). In 2000, Salager, Graciaa, et al. first published the equation known as the HLD (Salager, Marquez, et al., 2000). In 2007, Queste, Salager, Stray, and Aubry extended the relationship between HLD and EACN of oils (Questo et al., 2007). In 2008, Acosta published his initial work on HLD-NAC with nonionic surfactants (Acosta, 2008). In 2009, Kunz, et al. established the correlation between curvature, packing parameter, and HLD (Kunz et al., 2009). In 2020 Salager et al. revisited the HLD equation in its original form, by using a unit coefficient in the alkyl chain number (ACN) of the oil, introducing the so-called normalized HLD or  $HLD_N$  (Aubry et al., 2020; Salager et al., 2020), which allows its use in surfactant mixtures and understanding better the effect of each parameter by using the surfactant contribution parameter (SCP) (Salager, 2021; Salager, Graciaa, & Marquez, 2022; Salager, Marquez, & Ontiveros, 2022). It is crucial to note that there is some correspondence between HLD,

packing parameter and curvature, even if they are different concepts as noted by Kunz et al. (2009). This is in controversy with some studies calling the surfactant parameter in the HLD equation a "characteristic curvature" (Acosta et al., 2008; Leng & Acosta, 2023), when in other publications the surfactant parameter is said to be different from a measure of curvature (Salager, Graciaa, et al., 2022; Salager, Marquez, Rondón, et al., 2023). Tartaro et al. (2023) measured the curvature of a SOW system, clearly showing that the curvature not only depends on the surfactant but also on other variables such as the type of oil and temperature.

Determining the optimum formulation and applying the HLD equation can be straightforward for simple systems. However, for more complex systems, additional variables such as surfactant concentration and the water-oil ratio must be considered (Ontiveros et al., 2013; Salager et al., 2020). This is particularly relevant when using ternary SOW diagrams or when altering the formulation or surfactant concentration. Other representations, such as the "fish diagram," can provide further insights into these systems, related to solubilization (Questo et al., 2007; Salager et al., 2020), which was found to have a relationship with interfacial tension according to the Chun Huh correlation (Huh, 1979).

At the point where  $HLD_N$  equals zero, there are different measurements that can help to determine the optimum formulation. These include the phase behavior of the SOW systems, which can be assessed by measuring the volumes of the phases. When the quantities of oil and water phases solubilized in the surfactant-rich middle phase are considered, the optimum formulation can be identified (Marquez, Antón, et al., 2019; Pouchelon et al., 1980; Tartaro et al., 2023). Since the late 1970s, it has been observed that in model systems with pure ionic surfactants and pure oil phases, an equal partitioning of the surfactant between the oil and water excess phases is achieved at the optimum formulation (Salager, 1977; Salager, Morgan, et al., 1979; Wade et al., 1978). However, this is only the case for model systems because of a possible activity coefficient different from unity in real cases, in particular ethoxylated species. When more complex systems are studied, for instance, those involving a mixture of non-ionic surfactants or anionic surfactants that contain some impurities, the partitioning can be close to one between the two excess phases in the Will case, but not exactly one (Márquez et al., 1998; Salager, Márquez, et al., 2000; Salager et al., 1995). Consequently, the use of surfactant partitioning to determine the optimum formulation has not been widely adopted, as most of the real systems used in industry involve surfactant mixtures or oils that are not entirely pure.

Recent publications have also introduced other variables, such as interfacial elasticity, where a minimum is reached at the optimum formulation (Marquez, Forgiarini, Fernández, et al., 2018; Marquez, Forgiarini, Langevin, & Salager, 2018; Zamora et al., 2018). This is also

related to certain properties of the emulsified system, such as the minimum stability (Antón & Salager, 1986; Marquez et al., 2023; Marquez, Bullon, Forgiarini, & Salager, 2021; Marquez, Forgiarini, et al., 2019; Marquez, Meza, Alvarado, Johnny, et al., 2021). These techniques can be further extended with the use of other measurements that allow describing certain structural features of the domains present far away and around  $HLD_N = 0$ , among them, dynamic light scattering (DLS) and small angle scattering (SAXS and SANS) (Fukumoto et al., 2016).

The optimum formulation has several important applications in the physical chemistry of surfactant systems. One of these is the enhancement of solubility of certain substances, which is useful in various contexts. Another crucial application is in the creation of stable emulsions (far away from  $HLD = 0$ ) or in the destabilization of existing emulsions (exactly at  $HLD = 0$ ). Furthermore, surfactants can be characterized and optimized to modify and improve various processes. These are just a few of the uses of the optimum formulation in the context of surfactant systems, although one of the most widely used ones is the characterization of surfactants through the determination of the surfactant contribution parameter in the  $HLD_N$  equation, particularly for new surfactants, such as biobased and biosurfactants.

Herein, we review diverse methods to identify the optimum formulation in SOW systems. Section [Revisiting the methods to identify the optimum formulation is necessary to determine the SCP of biobased and biosurfactants](#) discusses the need to revisit the methods to identify the optimum formulation to characterize biobased and bio-surfactants. In Section [The optimum formulation concept](#), we aim to introduce the optimum formulation concept and comprehend the complexities of SOW systems. In Section [Winsor R ratio and HLD correlations](#), we discuss how to accurately quantify the changes in chemical potential with a multivariable linear equation, considering the effects of physicochemical formulation parameters. The concepts of the bicontinuous microemulsion, the formulation scan and formulation-composition map are presented in Sections [The bicontinuous microemulsion concept](#), [Formulation scans: A systematic method to determine the optimum formulation in SOW systems](#), and [Two-dimensional formulation-composition maps and the standard transitional inversion line](#). In Section [Optimum formulation detection methods](#), various methods to determine the optimum formulation are presented, along with a discussion of the advantages and disadvantages of each method. In Section [Phase behavior and minimum interfacial tension to detect the optimum formulation](#), we present some of the most used methods since the end of the 1970s, including the phase behavior and the minimum interfacial tension of equilibrated SOW systems. In Sections [Minimum emulsion](#)

[stability and viscosity to detect the optimum formulation](#), [Electrical conductivity of the emulsion](#), and [Oscillating spinning drop interfacial rheometer](#), we discuss measurements of emulsion properties to determine the optimum, such as the minimum stability, viscosity, electrical conductivity, and the dilational modulus measured with the Oscillating Spinning Drop Interfacial Rheometer (OSDIR). In Section [Complementary techniques that allow understanding of some structural features of the sow system around the optimum](#), we examine complementary methods to understand some structural features of microemulsions, with Section [Light scattering methods](#) focusing on light scattering methods such as DLS, and Small Angle X-Ray Scattering (SAXS). Sections [Nuclear magnetic resonance to Differential scanning calorimetry](#) discusses alternative approaches such as Nuclear Magnetic Resonance (NMR), x-ray micro-computed tomography (Micro-CT), and differential scanning calorimetry (DSC). The review concludes in Section [Complex cases for the determination of the optimum formulation](#) with final comments around complex behaviors, accuracy and application of some of the reviewed techniques, and a [Conclusions and Perspectives](#) Section.

## Revisiting the methods to identify the optimum formulation is necessary to determine the SCP of biobased and biosurfactants

In order to meet stringent environmental regulations and promote sustainability goals, industries are trying to reduce their reliance on conventional surfactants derived from fossil fuels. Instead, they are exploring the integration of new generation surfactants, such as biobased surfactants and biosurfactants (Hayes et al., 2019; Ortiz et al., 2022). The latter offer a compelling alternative to synthetic surfactants due to their reduced carbon footprint (Evonik, 2021; Kashif et al., 2022). As an example, substituting 1 metric tonne (Mt) of a typical ethoxylated surfactant with 1 Mt of sophorolipids, which are glycolipid biosurfactants, can result in a reduction of  $\sim 1.5$  Mt of  $CO_2$  emissions per metric ton of surfactant used (Bettenhausen, 2022). Nevertheless, according to cradle-to-grave analysis, first generation biosurfactants may not necessarily provide a significant improvement over other surfactant types in terms of sustainability (Bettenhausen, 2022). This is because first-generation biosurfactants are often derived from agricultural feedstocks, which can have a negative environmental impact if not managed properly. Factors such as land use, water consumption, and potential competition with food crops need to be carefully considered in assessing the overall sustainability of biosurfactant production (Kashif et al., 2022). On the other hand, biobased polyethoxylated surfactants are

being promoted as environmentally friendly, renewable and with low levels of 1,4-Dioxane (Croda, 2023). Ethylene oxide produced from biomass fermented into ethanol is carbon negative with a value of 0.6 kg of CO<sub>2</sub> per kg of ethylene oxide, but this number does not account for greenhouse gas emissions from growing the biomass (Bettenhausen, 2022).

Emerging biosurfactants, generally found in the form of complex mixtures, exhibit properties that are not completely predictable or well-understood, particularly when compared to their fossil fuel-derived synthesized counterparts (Hayes et al., 2019; Nguyen & Sabatini, 2011). For instance, biosurfactants that are currently being studied often underperform in applications requiring low interfacial tension or high solubilization (Kashif et al., 2022). The production costs associated with biosurfactants remain higher than those of their synthetic counterparts. This cost differential is primarily driven by the complexities involved in their extraction and purification processes (Gaur et al., 2022). To mitigate the economic challenges of biosurfactant production, researchers have shifted toward the utilization of lower-cost raw materials such as agricultural residues or agro-industrial waste.

There are only a few examples in the literature reporting surfactant contribution parameters (SCP) of biosurfactants (Nguyen & Sabatini, 2009). Given these factors, it becomes crucial to revisit the characterization methods to determine the surfactant parameters of new families of surfactants accurately. These include methods to determine the optimum formulation and to measure the SCP (also called  $\gamma$  or  $\beta$ ) in the Hydrophilic–Lipophilic Deviation (HLD) correlation or the Phase Inversion Temperature PIT-slope parameter (Aubry et al., 2020; Salager et al., 2020). Such parameters also enable tuning properties to formulate emulsions for specific applications (Delforce et al., 2023).

## The optimum formulation concept

Research on the formulation of SOW systems can be traced back to the mid-20th century. One approach considered to understand the changes in formulation involves comprehending the changes in chemical potential that occur in these systems (Aubry et al., 2020; Langevin, 2020; Lemahieu et al., 2022; Salager, Forgiarini, & Bullón, 2013). However, this is a challenging task, as it requires careful consideration of several compensating effects by each element of the system or by interactions with each other. Griffin's HLB was one of the first methods proposed to quantify the hydrophilic and lipophilic balance of surfactants with a single number (Griffin, 1949, 1954), but it is based on arbitrary assumptions and does not account for certain trends and variables such as temperature, salinity, among other characteristics of the system.

Winsor proposed the basic concepts of physicochemical formulation 70 years ago to correlate the phase behavior of SOW systems with the relative interactions of the surfactant molecules adsorbed at the interface with oil and water (Winsor, 1954; Winsor, 1968). While Winsor's model describes in a simple way how the surfactant, oil, and water interactions affect the physicochemical formulation, its application can be complex in practice (Langevin, 2020; Salager, Forgiarini, Márquez, et al., 2013; Salager, Márquez, & Ontiveros, 2022). According to Winsor's model, SOW systems can be classified into three types of equilibrated systems: Winsor I ( $R = A_{co}/A_{cw} < 1$ ), Winsor II ( $R = A_{co}/A_{cw} > 1$ ), or Winsor III ( $R = A_{co}/A_{cw} = 1$ ), based on the ratio  $R$  of surfactant ( $C$ ) molecules affinities for oil ( $O$ ) and water ( $W$ ), where  $A_{co}$  and  $A_{cw}$  are the molecular interactions between the adsorbed surfactant molecule and the nearby oil and water molecules. Winsor I systems correspond to type S1 micellar aggregation of surfactant molecules, eventually with some oil molecules solubilized inside, in what is called a swollen micelle. Winsor II systems correspond to type S2 inverse micelles, that is, the opposite structure of aggregation of surfactants in the oil phase, eventually with some water solubilization in their core (Israelachvili et al., 1976; Nagarajan, 2002). Winsor III systems, in which the interactions between surfactant and oil and water are equal, exhibit a three-phase behavior with a middle phase (Bourrel & Schechter, 2010; Scriven, 1977), which have been represented by Scriven as a bi or tri-continuous structure with very complex shapes containing oil and water fluctuating domains, looking as arbitrary "sponge" geometry or other unusual models (Scriven, 1976, 1977). While this phase has been commonly referred to as "microemulsion," it is noteworthy that there are no emulsion droplets present (Reger et al., 2012; Scriven, 1976, 1977) nor micrometer size objects, and consequently, the term is probably misleading as discussed by several researchers (Salager, Marquez, Rondon, et al., 2023) including one of the coauthors of Schulman initial paper (Prince, 1977).

In the 1970s, the rising price of crude oil led to research and development efforts aimed at increasing the final oil recovery above the typical 30% of the original oil in place (OOIP) after waterflooding (Bansal & Shah, 1977). It was found that the capillary trapping of oil could be eliminated by significantly reducing the Interfacial Tension (IFT) below 0.001 mN/m (Cash et al., 1977; Cayias et al., 1976; Miller et al., 1977; Shah & Schechter, 1977). This was happening in the  $R = 1$  case reported by Winsor (Marquez, Forgiarini, Langevin, & Salager, 2018; Salager, 1977; Salager, Bourrel, et al., 1979). This led to the study of the optimum formulation using a set of formulation variables, including (i) the salinity of the aqueous phase (brine) (Puerto & Gale, 1977), (ii) the nature of the crude oil (Salager, 1977), (iii) the temperature of the system

(Shinoda & Sagitani, 1978) (these three related to the physicochemical characteristics of the petroleum reservoir and its fluids), (iv) surfactant type (Bourrel et al., 1980; Salager, Morgan, et al., 1979), and (v) type and concentration of cosurfactants (Salager, Bourrel, et al., 1979). These variables could be adjusted based on the reservoir conditions, as well as the desired properties of the SOW system.

## Winsor R ratio and HLD correlations

The original R relationship provides a basic understanding of the formulation issues involved in phase inversion but is difficult to use in practice due to the complexity of determining the interaction parameters  $A_{co}$  and  $A_{cw}$ . In 1957, Davies introduced a correlation between the HLB value and the partitioning of surfactants between water and oil phases:  $HLB-7 = 0.36 \ln(C_W/C_O)$  (Davies, 1957), based on the free energy transfer of a surfactant molecule from water to oil (Equation 1):

$$\Delta G_{W \rightarrow O} = RT \ln \frac{C_W}{C_O}, \quad (1)$$

in which the  $C_W$  and  $C_O$  are the surfactant concentrations, often supposed to be as their activities in water and oil, respectively, because of near unity activity coefficients. Shinoda later used this correlation to explain the linear relationship between the change in phase inversion temperature (PIT) and ethyl oxide number (EON) of nonionic polyethoxylated surfactants (Shinoda, 1967).

In the early 1980s, the surfactant affinity difference (SAD) was originally defined as the difference between the negative standard chemical potential of the surfactant in the oil phase ( $\mu_O^*$ ) and the corresponding term for the water phase ( $\mu_W^*$ ), that is (Equation 2) (Marquez et al., 1995; Salager, 1996),

$$SAD = -\mu_O^* - (-\mu_W^*) = \mu_W^* - \mu_O^*. \quad (2)$$

Assuming that the activity coefficient is unity, which can be explained by the low surfactant concentration found in the excess phases of Winsor type III systems (i.e., CMC in the aqueous excess phase), then the equilibrium between the water and oil phases can be written in terms of the chemical potentials of the surfactant (Equation 3) (Marquez et al., 1995):

$$\mu_W = \mu_O = \mu_W^* + RT \ln \frac{C_W}{C_{W(ref)}} = \mu_O^* + RT \ln \frac{C_O}{C_{O(ref)}}, \quad (3)$$

in which the asterisk denotes the standard chemical potentials, whereas the subscript ref represents the

concentration references. If the partition coefficient between the aqueous and oil phases is defined as  $K = C_W/C_O$ , then (Equation 4):

$$RT \ln K + \text{constant} = \mu_O^* - \mu_W^* = \Delta G_{(W-O)} = -SAD. \quad (4)$$

The constant is the partition coefficient between the two reference states. The value of this constant does not matter since it does not change with the formulation variables that influence the standard chemical potentials.

The SAD is based on the difference between the numerator and denominator of the R relationship,  $R = A_{co}/A_{cw} = 1$ , that could be then expressed in an equivalent way as (Equation 5):

$$SAD = A_{co} - A_{cw} = 0. \quad (5)$$

The SAD has the advantage of being easier to calculate than other formulation semi-empirical equations because it involves the summation and subtraction of chemical potential terms rather than their ratio (Salager, 1996; Salager et al., 2020). Then, at the end of the 1990s, the concept of HLD was introduced as a generalized formulation dimensionless criterion (Salager, 1977; Salager, Márquez, et al., 2000), which can be expressed as (Equation 6):

$$HLD = \frac{SAD}{RT} = -\frac{\Delta G_{(W-O)}}{RT} = \frac{1}{RT} (\mu_W^* - \mu_O^*) = \ln K + \text{const} \quad (6)$$

in which  $R$  is the ideal gas constant and  $T$  is the temperature in Kelvin. The partition coefficient  $K = C_W/C_O$ , and the constant term (const), on the right side of the equation, correspond to the reference parameters chosen for the equation (e.g.,  $T_{ref} = 25^\circ\text{C}$ ,  $ACN_{ref} = 0$ , etc.).

The term  $\ln K$  can be correlated with the formulation variables, in a linear relationship very similar to HLD expression (Salager, 1996), by measuring the partition coefficient with different systems varying the type of oil, surfactant characteristics, alcohol content, brine salinity, and temperature. This approach works for ionic surfactants but it is completely different for nonionics which can present a distribution of molecular weights and partitioning can occur, thus, making it difficult to calculate the coefficients of the  $K$  expression (Marquez et al., 1995; Salager, Márquez, et al., 2000). Therefore, the change in the optimum formulation is made with two formulation changes in the HLD equation through formulation scans (Salager, 2021; Salager et al., 2020; Salager, Forgiarini, & Bullón, 2013), as will be shown in the following section.

## The bicontinuous microemulsion concept

When dealing with SOW systems, the phase equilibrium situations described by Winsor represent merely a

portion of the observable phenomenology. Liquid crystalline phases can be found even at low surfactant content and depending on the order of component addition and mixing procedure, meaning that they might not be at a real equilibrium. Winsor's WIII case involves true liquid phases: aqueous solution, oil solution and a liquid phase containing substantial quantities of water, oil, and almost all the surfactants.

The term microemulsion was introduced by Schulman et al. (1959) to define any thermodynamically stable, transparent, isotropic, liquid SOW system. Being transparent, the oil and water domains in the microemulsion must have sizes at least 10 times smaller than the visible light wavelength. The measurement of the self-diffusion coefficients of water ( $D_w$ ), oil ( $D_o$ ), and surfactant ( $D_s$ ) is likely to be the most straightforward way to assess the middle phase structure (Lindman et al., 2020). In the case of a swollen micelle WI solution,  $D_s \approx D_{oil} \ll D_w$ , while in the case of a swollen inverse micelle WII solution  $D_w \approx D_s \ll D_{oil}$ . In the case of a bicontinuous middle phase, the diffusion coefficients of the three components are uncorrelated, but water and oil have diffusion coefficients of the same order of magnitude as those of pure components (Tartaro et al., 2023). In the case of bicontinuous microemulsions (at  $HLD = 0$ ), there is no defined geometrical parameter describing the shape of the domains.

There is a body of knowledge with diverse explanations and models on the bicontinuous microemulsions subject, and there are uncertainties in relation to these models and interpretations. While not detailed herein, the different proposed models can be explored in the literature (Bourrel & Schechter, 2010; Hyde et al., 1997; Langevin, 2020; Salager, Marquez, Rondón, et al., 2023). In one of the models proposed by De Gennes, the degree of flexibility of the surfactant film can be described by a correlation length  $\xi$  (Tartaro et al., 2023). Such a correlation length can be measured by SAXS experiments, and it can be evaluated from the water and oil volume fractions and the amount of surfactant. According to the publication by Jouffroy et al. (1982), a bicontinuous microemulsion can be described using a lattice model of cubes of size  $\xi$  randomly filled by water and oil. Interestingly, techniques such as SAXS allow obtaining structural information of the microemulsion, indicating that at the optimum formulation, the correlation length  $\xi$  reaches a maximum for the bicontinuous microemulsion. The maximum in  $\xi$  corresponds to the state in which the middle phase solubilizes equal amounts of water and oil (Tartaro et al., 2023). Numerous publications have explored the concept of bicontinuous microemulsion, each with varying assumptions. Therefore, a comprehensive review of the existing literature is necessary to gain a more complete understanding of the topic (Gradzielski et al., 2021; Hyde et al., 1997; Scriven, 1977).

## Formulation scans: A systematic method to determine the optimum formulation in SOW systems

Formulation scans are a widely used technique for systematically altering the physicochemical interactions between surfactant, oil, and water in SOW systems. These scans involve changing variables that can affect the formulation, such as salinity, surfactant (head and tail) type, oil alkane carbon number ACN, temperature, and pressure (Ghosh & Johns, 2016; Pouchelon et al., 1980; Salager et al., 2010; Salager, Forgiarini, Márquez, et al., 2013). While effectively used to identify the optimum formulation, this technique can be very time-consuming if not performed wisely. Consequently, unidimensional scans, which consist in altering a single variable at a time, can serve as an efficient means to identify the optimum formulation at a minimum interfacial tension (Aubry et al., 2020; Cayias et al., 1976; Sottmann & Strey, 1997).

Ternary SOW diagrams have been found to change with the multivariable formulation, which can be regarded as a six variable equation, and can be described mathematically with a single generalized expression recently proposed (Aubry et al., 2020; Forgiarini et al., 2021; Salager, 2021; Salager et al., 2019, 2020), the so-called Normalized Hydrophilic-Lipophilic Deviation ( $HLD_N$ ) that has the same ACN variation unit in all cases (Equation 7) (Aubry et al., 2020; Salager et al., 2020; Salager, Forgiarini, Márquez, et al., 2013):

$$HLD_N = SCP \text{ (or PACN)} - ACN + k_S \ln S \text{ (or } k_S S) - k_A C_A \pm k_T (T - T_{ref}) - k_P (P - P_{ref}) = 0, \quad (7)$$

where the  $ks \ln S$  or  $ks S$  terms are used when ionic or nonionic surfactants are present in the system, respectively. ACN is the alkane carbon number when the oil is an *n*-alkane or EACN when it is another oil (Queste et al., 2007), *S* is the salinity expressed as wt%/vol% of NaCl,  $C_A$  is the alcohol concentration (wt%/vol%), *T* is the temperature (°C) and *P* the pressure (atm). The numerical value for the constants  $k_S$ ,  $k_A$ ,  $k_T$ , and  $k_P$  can be found elsewhere (Salager, 2021). The  $HLD_N$  simplifies the HLD equation by dividing it by the coefficient  $k_{ACN}$  of the ACN variable. This allows the surfactant parameter for both anionic and nonionic surfactants to have the same reference ( $\sigma$  and  $\alpha$ -EON from ionic and ethoxylated nonionic surfactant HLD equations, respectively) and be expressed as a Surfactant Contribution Parameter (SCP or PACN; Aubry et al., 2020; Ontiveros et al., 2018), for ionic or nonionic surfactants. The  $HLD_N$  equation is useful to determine the optimum formulation of simple SOW mixtures and understand complex systems, as in the case of enhanced oil



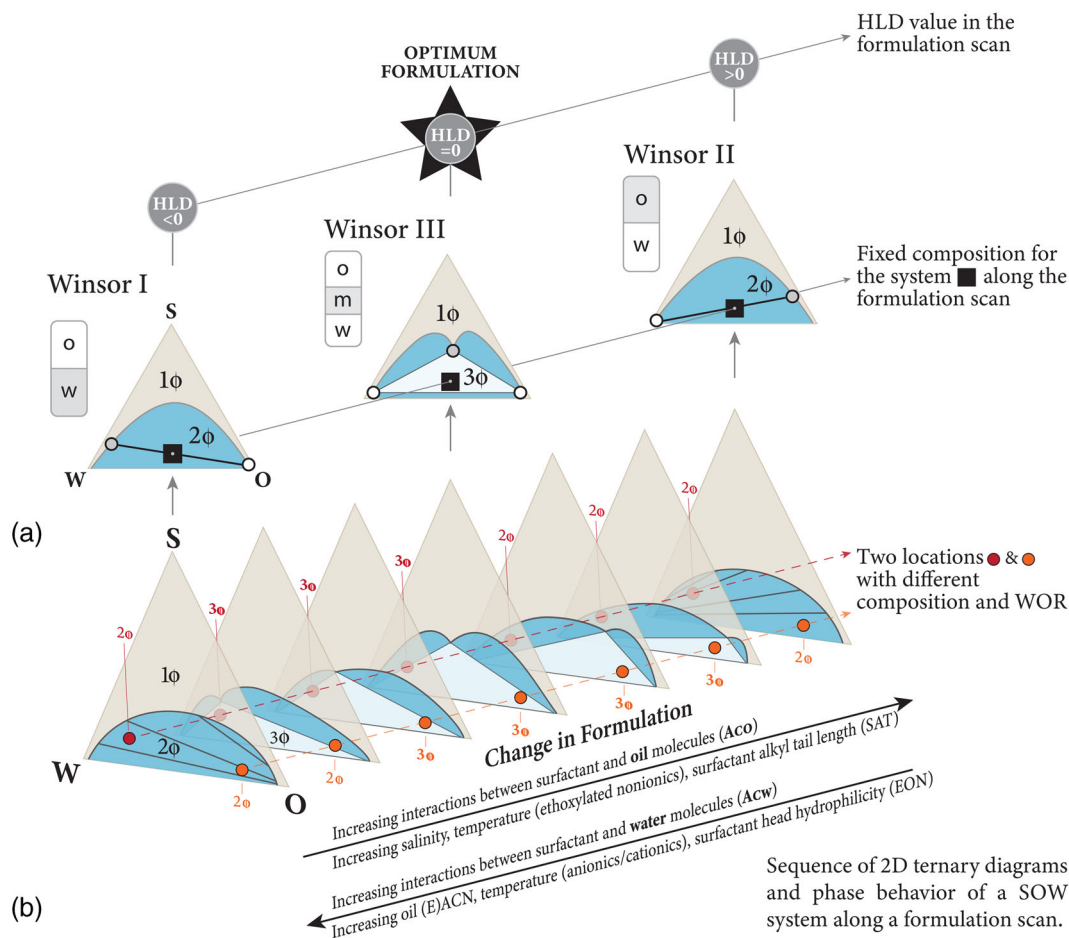


**FIGURE 1** (a) Variation on the Winsor ternary diagram when a formulation change occurs (salinity here, but also occurring with temperature, ethyl oxides number EON, alkyl chain number ACN, etc.). (b) The morphological changes and the variation in the Winsor III triphasic zone in a surfactant–oil–water (SOW) system upon changes in formulation, surfactant concentration and WOR. At different composition points the morphology of the system can change according to the formulation and WOR: At a surfactant concentration below the  $x$  point bicontinuous (Winsor III) microemulsions can be attained, while over that point a monophasic phase is formed.

recovery, detergency, dewatering, or emulsification applications, where surfactant mixtures are often necessary (Salager, Forgiarini, Márquez, et al., 2013).

In a SOW system, slight changes in the formulation can result in a shift in the phase behavior at the same composition point in a ternary diagram (Figure 1). This can lead to a change in the optimum formulation, which is typically characterized by a minimum tension or a three-phase behavior with equal amounts of excess phases. Figure 1 depicts the changes in the ternary diagram when the formulation (e.g., salinity) is altered. Surfactants tend to partition preferentially to one of the phases, such as the water phase at low salinity or the oil phase at high salinity. The optimum formulation is usually attained when the surfactant forms a third intermediate (middle) phase with bicontinuous structure (Salager, Forgiarini, et al., 2002).

The previous Figure 1a is the representation in 2D of the ternary diagram. Then in Figure 1b, we observe the changes within the Winsor III middle zone as a function of formulation, WOR, and surfactant

concentration in a 3D diagram. The middle phase is attained at different values of the formulation variable, depending on the surfactant, oil, and water ratios. It is worth noting that the optimum value of the formulation variable is influenced by the WOR and surfactant concentration. This is important for different applications, including enhanced oil recovery (EOR), in which the typical WOR is in the range of 3–4, and crude oil dehydration, in which the WOR is  $\sim 0.1$ –0.2, as well as in food, cosmetics, and paints, in which the WOR may vary significantly from one to another (Wasan & Mohan, 1977).

Although Will equilibrated systems at optimum formulation have been traditionally characterized by a minimum interfacial tension and a three-phase behavior at a fixed surfactant concentration and oil-to-water ratio, several reports show that a number of other characteristic properties can be taken into account (Figure 2), such as a minimum in dilational interfacial rheology (Marquez, Forgiarini, Fernández, et al., 2018; Marquez, Forgiarini, Langevin, & Salager, 2018), emulsion

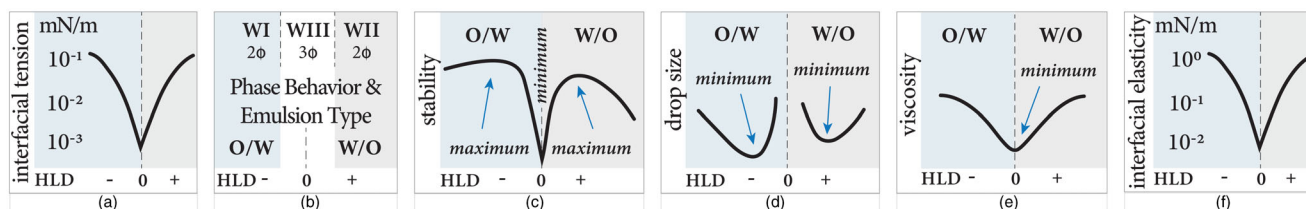


**FIGURE 2** Property changes near the optimum formulation (HLD = 0). (a) Interfacial tension, (b) emulsion type and inversion, (c) emulsion stability, (d) droplet size, (e) viscosity, and (f) dilational modulus.

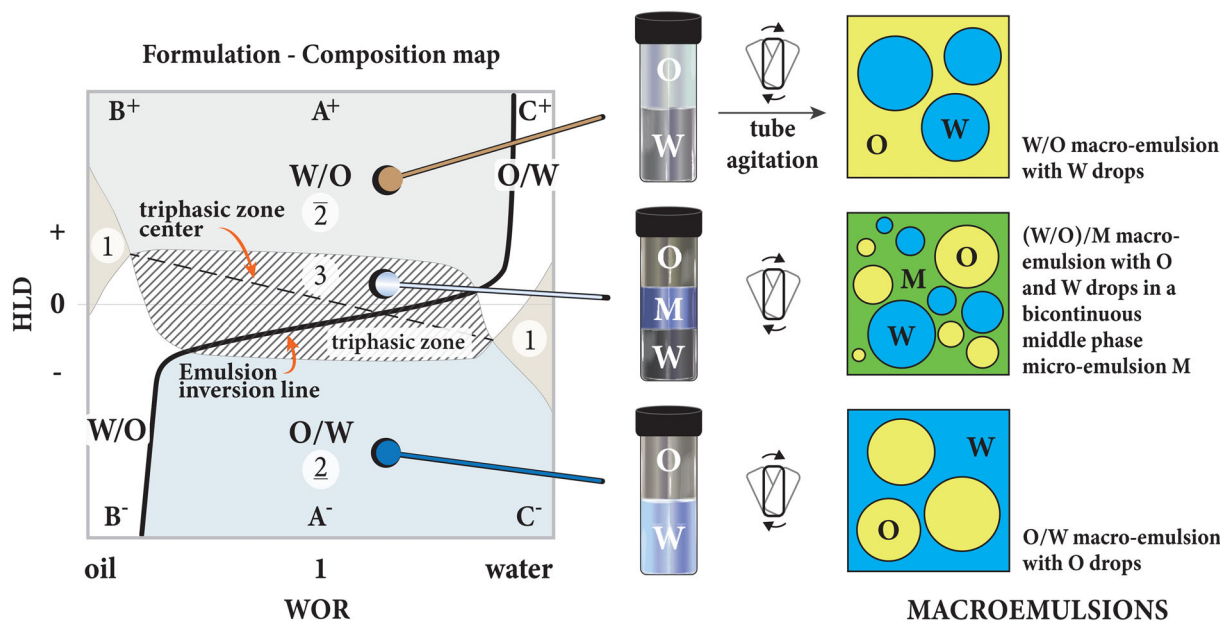


**FIGURE 3** Formulation-composition map showing the different zones where normal and inverse emulsions are found.  $A^-$  and  $C^-$  zones indicate normal O/W emulsions, while  $A^+$  and  $B^+$  represent inverse emulsions.  $B^-$  and  $C^+$  are called the abnormal zones, where multiple emulsions can be formed. The somber zone in the middle represents the three-phase behavior zone. The black line in the center represents the transitional emulsion phase inversion, and the slashed line represents the catastrophic inversion line. The right panel depicts a schematic representation of the macroemulsion morphology when the test tube systems are agitated.

electrical conductivity jump (Salager et al., 1982), minimum in emulsion viscosity (Salager, MiñanaPerez, et al., 1983) and stability (Salager, Miñana-Pérez, et al., 1983; Vinatieri, 1980), light transmission and backscattering, among others (Antón et al., 1986; Lemahieu et al., 2021; Miñana-Pérez et al., 1999; Pierlot et al., 2016, 2019; Rout et al., 2012; Salager et al., 1990; Salager, Miñana-Pérez, et al., 1983). Some of these methods used the close relation between the phase behavior at equilibrium and the emulsion morphology when these systems are agitated to relate the optimum formulation of the equilibrated systems to the phase inversion of the corresponding emulsions (Pizzino et al., 2007, 2013; Schirone et al., 2022). In addition, other phenomena occur at a distance from HLD = 0, for example, minimum droplet size and stability (Antón & Salager, 1986; Salager, 2000; Tolosa et al., 2006). Although the situation at HLD = 0 is often associated with minimum

interfacial tension and maximum solubilization in the middle phase, the actual value can vary according to the specific formulation and system conditions. Therefore, the interfacial tension and other variables (shown in Figure 2c–f) can be influenced also by other factors including surfactant concentration, oil and water properties type of salt (Vera et al., 2020), oil type (Ontiveros et al., 2013), and temperature (Salager, Forgiarini, & Bullón, 2013; Salager, Forgiarini, Márquez, et al., 2013).

### Two-dimensional formulation-composition maps and the standard transitional inversion line

A formulation-composition map (Miñana-Pérez et al., 1986) is a graphical representation of the relationship between a formulation variable (HLD) and the water or oil fraction

that influences the properties of an emulsion, such as its morphology (oil-in-water or water-in-oil), droplet size, viscosity, and stability. The formulation-composition map can be divided into six regions based on the HLD value and the water or oil content (i.e.,  $A^-$ ,  $B^-$ ,  $C^-$  and  $A^+$ ,  $B^+$ ,  $C^+$ ), as shown in Figure 3.

When the WOR value is close to the unity, the physicochemical formulation determines the emulsion morphology and is referred to as “normal.” The almost horizontal inversion branch (black line) follows the optimum formulation from conductivity, indicating that the emulsion’s morphology is determined by the properties of the mixture in this region (i.e.,  $A^-$  and  $A^+$ ). The almost horizontal dashed line is the tension minimum that is more or less at the center of the three-phase zone. A change in the morphology of a “normal” W/O emulsion (in  $B^+C^+$ ) from one side of the  $HLD = 0$  zone, to the other side of “normal O/W emulsion (in  $A^-C^-$ ),” is called a “transitional inversion.” However, when the HLD value is slightly higher than zero (for W/O emulsions), or slightly less than zero (for O/W emulsions) and the internal phase content is quite high or quite low, the emulsion is considered “abnormal,” that is contrary to the normal expectation and it may exhibit multiple emulsion characteristics (in  $B^-$  and  $C^+$ ). The inversion line’s vertical and sometimes slanted branches on the map mark the transition from normal to abnormal emulsions, referred to as “catastrophic” due to its sudden occurrence. In other words, when HLD is significantly greater or less than 0, the normal emulsion becomes W/O or O/W, respectively, until a high proportion of the internal phase is reached. Beyond this point, the emulsion inverts and becomes “abnormal.” The butterfly catastrophe model (Salager, 1985, 1988) explains both types of emulsion inversion based on the properties of the mixture and the composition of the surfactant and water–oil ratio. It is widely accepted as the most accurate model for understanding the complexity of emulsion inversion (Salager, Marquez, et al., 2000). It is seen in Figure 3 that the fact that the solid and dashed line are not coinciding exactly produces some confusion to determine what is the  $HLD = 0$  location.

One concept that has been extensively studied in the context of emulsion stability is the standard inversion line. The transitional inversion locus represents the boundary between stable and unstable emulsions and can be used to predict the conditions under which an emulsion will undergo inversion. The first article in which the term “standard” inversion frontier or line appeared delineated the sets of conditions that result in an O/W and a W/O region on an appropriate formulation-composition map (Salager, Marquez, et al., 2000; Salager, Miñana-Pérez, et al., 1983). Surfactant composition and concentration can also affect the position of the inversion boundary through surfactant partitioning between the phases and alteration of

the distribution of lipophilic and hydrophilic oligomers at the droplet interface (Galindo-Alvarez et al., 2011).

## OPTIMUM FORMULATION DETECTION METHODS

The most common method used to identify the optimum formulation involves preparing a series of test tubes with different formulations, shaking them gently, and then observing which one causes an excess phase (W or O) to separate the fastest. It is a measurement of the immediate instability of one emulsion produced. It must be said that it is not a scientific method with a number to quantify but an almost instantaneous guess.

This conjecture is advantageous because the optimum formulation is typically located at or very close to the point at which an excess phase starts to appear, which corresponds to the stability minima in Figure 2, indicating the lowest stability for O/W and W/O emulsions (Antón & Salager, 1986; Marquez, Forgiarini, Langevin, & Salager, 2018), or for both at the same rate in fortunate cases exactly at  $HLD = 0$ . However, it should be noted that although this method is simple and easy to measure, the underlying phenomena are complex (McClements, 2007; Tolosa et al., 2006), and a thorough understanding of formulation principles and surface properties become relevant (Langevin, 2020; Salager, 2006).

Previous studies have also demonstrated that the apparent equilibration of the emulsified system occurs very rapidly, often immediately, near the optimum formulation (Salager, Moreno, et al., 2002). This separation does not depend on the water-to-oil ratio (WOR) or surfactant concentration (unless a viscous liquid crystal phase is formed). The undisputable determination of optimum formulation is performed with the minimum interfacial tension measurement, which is detailed in Section [Phase behavior and minimum interfacial tension to detect the optimum formulation](#). The optimum formulation is also determined indirectly by the stability or viscosity measurement of agitated systems (Pizzino et al., 2013) (Section [Minimum emulsion stability and viscosity to detect the optimum formulation](#)). Electrical conductivity (Section [Electrical conductivity of the emulsion](#)), the minimum in interfacial dilational modulus (Section [Oscillating spinning drop interfacial rheometer](#)), and other complementary techniques that allow understanding some structural features of the SOW system around the optimum, such as wave scattering techniques: DLS and small angle scattering (SAXS and SANS) (Section [Light scattering methods](#)), NMR, X-ray microcomputed tomography (Micro CT), and differential scanning calorimeter (DSC) (Section [Nuclear magnetic resonance](#)). The advantages and inconveniences of each method and the particular cases are discussed. Table 1 presents a summary of each method reviewed

**TABLE 1** Methods to measure the optimum formulation in surfactant–oil–water systems and methods to obtain an understanding of the structural features of the surfactant-rich phase in SOW systems.

Method	Variable measured	Principle of measurement	Measurement range	Advantages	Limitations
<b>Minimum interfacial tension</b>	Interfacial tension between two phases, including if three are present	Spinning drop method. Equilibrium of forces between the two phases, the droplet (less dense) and the bulk (denser)	$10^{-4}$ to 10 mN/m Droplet volume: 0.5–5 $\mu\text{L}$ . Rotational speed at low IFT: 3000–6000. Equilibration time: 1 min–1 h	<ul style="list-style-type: none"> <li>- Accurate measurement of interfacial tension.</li> <li>- Is the undisputable method to determine the optimum formulation.</li> </ul> Can be used for a wide range of interfacial tension values	<ul style="list-style-type: none"> <li>- Limited to measuring interfacial tension of two immiscible fluids.</li> <li>- Cannot detect emulsion inversion or stability directly.</li> <li>- Several tubes in a formulation scan are needed to reach equilibrium. It is time consuming, several tensiometer are needed to make faster scans.</li> </ul>
<b>Electrical conductivity</b>	Conductivity of emulsified system	Electrical conductivity of the emulsion changes upon inversion of the emulsion.	$10^{-6}$ to $10^{-3}$ S/m	<ul style="list-style-type: none"> <li>- Can be used to identify the inversion point of an emulsion quickly.</li> <li>- Simple and fast measurement</li> </ul>	<ul style="list-style-type: none"> <li>- Limited to detecting phase inversion.</li> <li>- May be depending on the stirring energy and electrode wettability</li> </ul>
<b>Viscosity</b>	Viscosity of emulsified system	Resistance to flow of (homogeneous) emulsion	0.1 to 1000 mPa s	<ul style="list-style-type: none"> <li>- Provides valuable information on flow behavior of emulsions.</li> <li>- Does not require special preparation of the sample.</li> </ul>	<ul style="list-style-type: none"> <li>- The sample volume should be enough to perform a viscosity test.</li> <li>- Not able to detect stability of emulsion. Depending on the formulation variable, several samples are needed to determine the optimum formulation.</li> </ul>
<b>Minimum emulsion stability</b>	Emulsion stability	Time it takes for emulsion to separate into two (or three) phases, that is, lifetime of emulsions. Usually measured as the time required to separate 50% of the internal phase.	Seconds, hours to days	<ul style="list-style-type: none"> <li>- Provides information on the stability of emulsions, critical in various applications.</li> </ul>	<ul style="list-style-type: none"> <li>- Test may not be able to detect small changes in emulsion stability.</li> <li>- Difficult to measure for opaque or dark phases.</li> </ul>
<b>Minimum dilatational interfacial modulus</b>	Dilatational modulus (E)	Dilatational modulus of the interface for an elongated droplet under constant oscillation in a spinning drop apparatus.	$10^{-3}$ to 10 mN/m Droplet volume: 0.5–5 $\mu\text{L}$ . Rotational speed at low IFT: 3000–6000. Equilibration time: 1 min–1 h	<ul style="list-style-type: none"> <li>- Provides information of the surfactants molecules adsorbed at the interface on the interfacial film properties.</li> <li>- Allows measurement for a range of frequency change values.</li> </ul>	<ul style="list-style-type: none"> <li>- Measuring the dilatational modulus in very low interfacial tension systems under oscillation is challenging due to the very low diameter of the droplet.</li> <li>- Same limitations as the spinning drop apparatus</li> </ul>

TABLE 1 (Continued)

Method	Variable measured	Principle of measurement	Measurement range	Advantages	Limitations
<b>Dynamic light scattering (DLS)</b>	Light scattering	The diffusion coefficient of particles reaches its maximum value approaching the optimum formulation in single phase colloidal solutions	0.3 nm to 1 $\mu$ m	<ul style="list-style-type: none"> <li>- Can provide information on the size and distribution of micelles at the sides of the optimum.</li> <li>- Fast and non-destructive measurement technique.</li> </ul>	<ul style="list-style-type: none"> <li>- Measures particles in the nanometer to sub-micrometer size range.</li> <li>- DLS assumes that particles in a sample are of uniform size and shape.</li> <li>- Transparency: If a sample is highly opaque or contains a large number of impurities, this can interfere with the accuracy of the measurements.</li> </ul>
<b>Small angle x-ray scattering (SAXS)</b>	X-rays scattering	At the optimum formulation, the Teubner and Stray (T-S) model fitting of the scattered intensity ( $I(q)$ ) reveals a minimum domain size ( $d$ ) and a maximum correlation length ( $\xi$ ).	0.1 nm to 1 $\mu$ m	<ul style="list-style-type: none"> <li>- Can provide valuable information on the size and shape of domains in a microemulsion.</li> </ul>	<ul style="list-style-type: none"> <li>- Low-resolution technique compared to other methods.</li> <li>- It cannot provide information about the internal structure or composition of the ME droplets.</li> <li>- Requires samples to be in a homogeneous and isotropic state, which may not always be possible for complex microemulsions with multiple phases or non-spherical droplets.</li> </ul>
<b>T1-weighted nuclear magnetic resonance (NMR)</b>	T1 relaxation times of two or three phase systems	The optimum formulation is determined based on the quantification of NMR profiles of the oil and water phase of the microemulsions.	10 to 100 ms	<ul style="list-style-type: none"> <li>- Can provide valuable information on the composition and physical properties of a microemulsion.</li> <li>- Non-destructive technique.</li> <li>- Able to measure a wide range of relaxation times.</li> </ul>	<ul style="list-style-type: none"> <li>- Limited sensitivity when compared to other techniques, such as T2-weighted NMR.</li> <li>- Limited resolution by the size of the NMR sample and the strength of the magnetic field.</li> <li>- Long acquisition times, which can be a disadvantage when studying microemulsions that are dynamic and undergo rapid changes over time.</li> <li>- Limited information since it does not provide the size or shape of the components.</li> </ul>

(Continues)

TABLE 1 (Continued)

Method	Variable measured	Principle of measurement	Measurement range	Advantages	Limitations
<b>X-Ray microcomputed tomography (micro-CT)</b>	Attenuation of X-rays of two or three phase systems	X-ray radiation is transmitted through the sample and a radiography showing the thickness of the different phases present in a microemulsion is used to quantify the optimum.	1 $\mu\text{m}$ to 10 mm	<ul style="list-style-type: none"> <li>- Provides detailed images of the internal structure of a sample.</li> <li>- Can handle a wide range of sample sizes.</li> <li>- Non-destructive technique.</li> </ul>	<ul style="list-style-type: none"> <li>- Spatial resolution limited by the X-ray source and detector, which may not be sufficient to resolve the internal structure of certain systems.</li> <li>- Limited contrast for systems with similar x-ray attenuation coefficients to their surrounding media.</li> <li>- Slow imaging technique.</li> <li>- Radiation damage leading to changes in the system's structure and composition.</li> </ul>
<b>Differential scanning calorimetry (DSC)</b>	Heat Flow to determine a change in structure	Measures the heat flow between a reference cell and a sample cell, where the sample cell contains the microemulsion. The temperature is then increased or decreased at a constant rate, and the heat flow is measured as a function of temperature.	-50 to 500°C	<ul style="list-style-type: none"> <li>- Can detect phase changes in a sample, which can provide valuable information on the thermal stability.</li> <li>- Able to handle a wide range of temperatures.</li> </ul>	<ul style="list-style-type: none"> <li>- The sample must be homogeneous.</li> <li>- Any impurities or contaminants in the sample can interfere with the DSC measurement.</li> <li>- DSC has limited resolution, which may make it difficult to detect small changes in the heat flow during a phase transition.</li> <li>- Cannot provide information on the structure or morphology of the microemulsion</li> </ul>

Note: Variable measured, principle and interval of measurements, advantages and limitations are presented for each method.

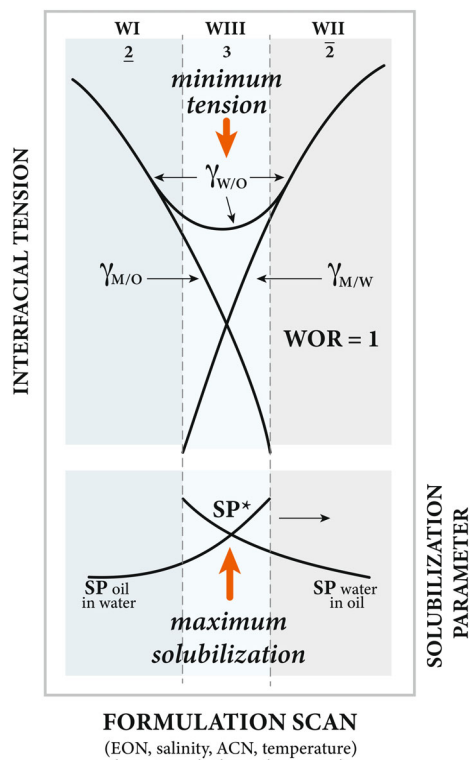


**FIGURE 4** Properties of equilibrated systems at optimum formulation: Minimum interfacial tension, which corresponds to the maximum solubilization  $WOR = 1$ , according to Chun Huh relation (Huh, 1979).

in the present work, the variable measured, principle, and interval of measurements, advantages, and limitations.

### Phase behavior and minimum interfacial tension to detect the optimum formulation

The detection of the optimum formulation for enhanced oil recovery (EOR) is often based on the measurement of the minimum interfacial tension at equilibrium (Figure 4), which corresponds to the desired increase in capillary number and displacement of crude oil. This measurement is considered the most relevant for the purpose of the application. However, obtaining this measurement can be a time-consuming process, as it requires allowing for equilibration over 1–2 days and the stabilization of low interfacial tension over minutes or hours when low diffusing species are in the mixture, such as polymeric surfactants or with crude oils containing a large percentage of asphaltenes that are heavy lipophilic surfactants. In certain cases, the interfacial tension may stabilize quickly, particularly in the presence of cosurfactants such as sec-butanol, which slightly affects the optimum formulation (Marfisi et al., 2005). Therefore, certain variables may contribute to rapid mass transfer in addition to the  $HLD_N = 0$

condition, including: (1) surfactant concentration without reaching the Winsor IV region (Rondón-González et al., 2006), which is the point where a homogeneous single phase system appears, and (2) the use of  $C_3$ – $C_5$  alkyl chain alcohols (Kim & Wasan, 1996).

According to the solubilization performance in a SOW system and the formation (or not) of a microemulsion bicontinuous middle phase with a large volume, the visual method to determine the optimum at the occurrence of equal solubilization of oil and water can be measured (or not) (Marquez, Antón, et al., 2019; Marquez, Forgiarini, Langevin, & Salager, 2018; Salager et al., 1982). In this section, we will describe two cases, on the one hand, the case where a low surfactant concentration and a small volume of middle phase is attained, and on the other hand, the case where a large volume of microemulsion middle phase is present.

### The case of a small volume of microemulsion middle phase

We will begin this section by describing how to determine the optimum formulation with interfacial tension measurement, when there is a low surfactant concentration and very little microemulsion middle phase. In Figure 5, a formulation scan of the sodium dodecyl benzene sulfonate (SDBS)/cyclohexane/brine system shows that the optimum formulation is attained at a salinity of 3.4 wt%, which was determined with a minimum of interfacial tension in Figure 5 right panel, and as evidenced with the  $HLD_N$  equation (Equation 8).

$$HLD_N = k_S \ln(S) + SCP \text{ (or PACN)} - EACN + k_T(T - 25), \quad (8a)$$

$$HLD_N = 6.25 \ln(S) + (-3.75) - 3.5 + (-0.0625)(30 - 25) = 0, \quad (8b)$$

where  $k_S = 6.25$ ,  $SCP = -3.75$ , and  $k_T = -0.0625$  for sodium dodecyl benzene sulfonate, and  $EACN = 3.5$  for cyclohexane, and  $T = 30^\circ\text{C}$ . When the salinity at optimum formulation,  $S = 3.4$  wt%, is substituted in the equation,  $HLD_N = 0$  is satisfied.

The challenge with these types of systems is that the microemulsion middle phase volume is very small due to the very low surfactant concentration (Marquez, Forgiarini, Langevin, & Salager, 2018). This is often the case in practical applications such as crude oil dewatering, enhanced oil recovery, and even detergency and cosmetic applications with low surfactant concentration restrictions due to cost reduction considerations (Marquez, Forgiarini, et al., 2019; Marquez, Meza,

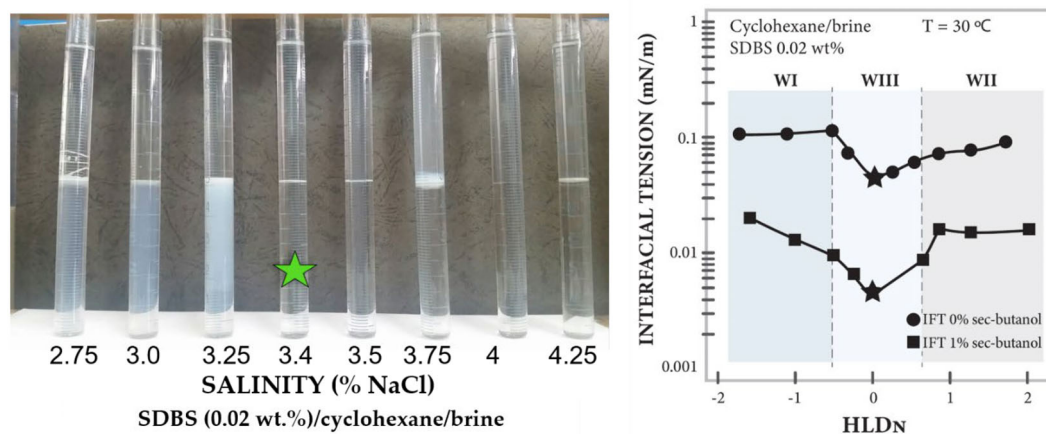


**FIGURE 5** Left: Phase behavior of the SDBS/cyclohexane/brine system at 0.02 wt% surfactant,  $T = 30^{\circ}\text{C}$ . Right: Interfacial tension minimum found at the optimum formulation (3.4 wt% NaCl) when measured with the spinning drop apparatus. Two cases are presented, the first when no sec-butanol is added to the system and very small solubilization is attained as indicated in the left panel figure. The second system contains 1 wt% sec-butanol, which generates higher solubilization and thus, a lower interfacial tension, according to Chun Huh relation (Huh, 1979). Source: Figure reproduced from Marquez, Forgiarini, Langevin, and Salager (2018).

Alvarado, Bullón, et al., 2021). Therefore, in cases where a small amount of microemulsion middle phase is formed, the optimum should be measured by the minimum of interfacial tension (Salager, Forgiarini, & Bullón, 2013), or in some applications such as crude oil dewatering, with the minimum of emulsion stability (Delgado-Linares et al., 2016).

Measuring low interfacial tension typically requires the use of specialized equipment such as a spinning drop tensiometer, and in practice, may involve multiple devices. For example, the Wade and Schechter Laboratory at the University of Texas had 25 such devices in the 1970s, which allowed them to generate over a hundred data points in a single day (Wade et al., 1978).

At water-to-oil ratios (WOR) very different from unity and at variable surfactant concentrations, partitioning of the surfactant species may occur, as in the case of commercial ethoxylated surfactants (Graciaa et al., 1987). Therefore, ensuring that the interface is at the optimum critical condition is crucial, as leaving the (partial) equilibration in a spinning drop tube can result in rapid or slow changes in tension or even complete solubilization of the drop due to the transfer of surfactant. Previous studies have shown that systems without alcohol reach equilibrium at lengthy times, exceeding 4 h, while systems with alcohols such as sec-butanol reach equilibrium in a shorter period (often less than 1 h) (Marquez, Antón, et al., 2019; Marquez, Forgiarini, Langevin, & Salager, 2018). This rapid exchange of surfactant at the optimum formulation, in which there is virtually no resistance to mass transfer by diffusion in the presence of sec-butanol, can affect emulsion stability, with the system containing sec-butanol having lower stability when compared with the system without alcohol (Marquez, Meza, Alvarado, Bullón, et al., 2021; Zamora et al., 2018).

### The case of a large volume of microemulsion middle phase

Conversely, when the surfactant concentration is sufficiently high and the system exhibits high performance and solubilization, a large volume of microemulsion middle phase can be attained (Figure 6) (Marquez, Antón, et al., 2019). In this case, we present a formulation scan of a sodium dodecyl sulfate (SDS) surfactant/kerosene/brine system, with 3% n-pentanol alcohol. It is evident that a large microemulsion volume system can be attained at 5.2 wt% NaCl. This suggests that the volume of the excess phases can be measured. Consequently, when the water-to-oil ratio equals 1, the point at which both phases are equally solubilized in the middle phase microemulsion can be determined visually, or even with other instrumental measurements such as NMR or Micro-CT, particularly when non-transparent systems are involved. Therefore, in this case, where a large volume of middle phase is attained, from a practical point of view, it is better to determine the optimum visually, rather than performing lengthy interfacial tension (IFT) measurements. When three phases are present IFT measurements should be performed carefully, for example, separating the bottom and top phases of the tubes, without extracting the middle phase to attain accurate measurements (Antón & Salager, 1986; Marquez, Antón, et al., 2019).

### Minimum emulsion stability and viscosity to detect the optimum formulation

It has been observed that emulsion stability and viscosity tend to be low at the optimum formulation (Boyd et al., 1972). This phenomenon was first observed in the



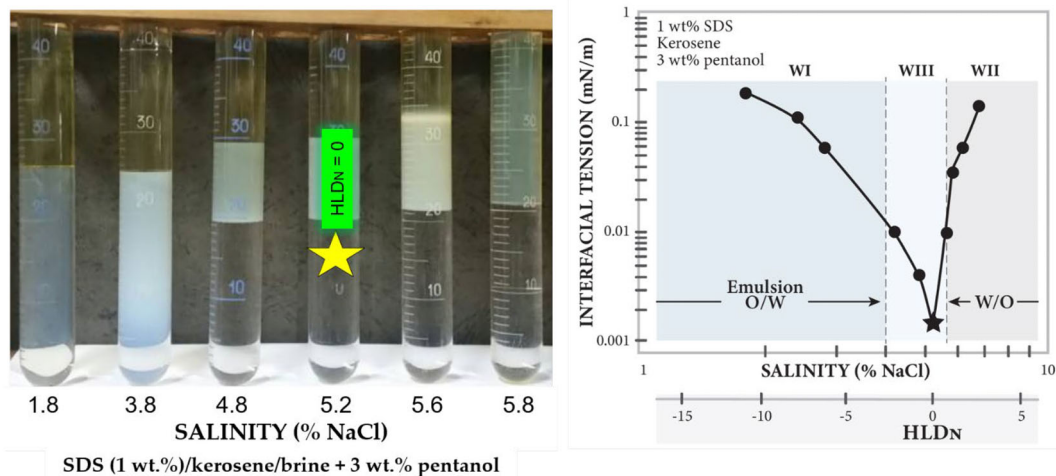


**FIGURE 6** Left: Interfacial tension minimum found at the optimum formulation (5.2 wt% NaCl) in the SDS/Kerosene/Brine system at 1 wt% surfactant and 3 wt% n-pentanol,  $T = 30^\circ\text{C}$ , when measured with the spinning drop apparatus. Right: Phase behavior of the system. The large solubilization that is attained is evidenced by the very low interfacial tension, according to Chun Huh relation (Huh, 1979). Source: Figure reproduced from Marquez, Antón, et al. (2019).

1970s and 1980s through the use of formulation scans (Miñana-Pérez et al., 1986; Salager et al., 1982). It has been demonstrated to occur for both oil-in-water (O/W) and water-in-oil (W/O) emulsions, as well as for oil-in-water-in-oil (O/W/O) systems (Antón & Salager, 1986). The low lifetime of emulsions at the optimum formulation has been discussed extensively in previous publications (Antón & Salager, 1986; Salager, Marquez, Delgado-Linares, et al., 2022; Marquez et al., 2018).

Winsor and Shinoda (Shinoda & Saito, 1969; Winsor, 1948, 1954) and other authors have noted that emulsion stability tends to decrease as the SOW system approaches the optimum formulation. However, it was only through several articles reporting formulation scans (Salager et al., 1982; Vinatieri, 1980) that a systematic relationship between the minimum stability of the emulsion and the optimum formulation was found. This relationship was further corroborated in subsequent studies (Graciaa et al., 1982; Milos & Wasan, 1982; Salager et al., 1982), including a measurement of the stability of the two-phase emulsion in the three-phase behavior, which was demonstrated by Antón and Salager (1986) as two minima of stability very close to the center of the WIII zone. High instability at the optimum formulation was justified from fundamental studies (Al-Sabagh, 2002; Kabalnov & Wennerström, 1996; Kiran & Acosta, 2015; Ruckenstein, 1996).

On the other hand, the minimum viscosity of an emulsion can be attributed to concurrent phenomena. While the viscosity of the internal phase does not significantly affect the overall viscosity of the emulsion, the internal phase content plays a significant role (Pierlot et al., 2016; Ramírez et al., 2002). The emulsion formulation may also affect viscosity, particularly when approaching the so-called optimum formulation (Figure 7). Indeed, when the

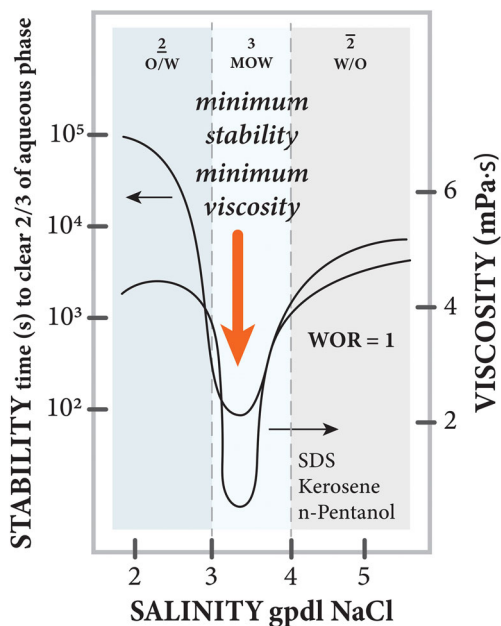


**FIGURE 7** Minimum emulsion stability and viscosity for emulsions near optimum formulation. In the right figure g/dl stands for grams per deciliter, units used in the 1980s in practice, corresponding to wt%/vol%. Source: Adapted from Antón and Salager (1986).

interfacial tension is low, the droplets within the emulsion tend to elongate, leading to a reduction in the interactions among them. As a result, the viscosity of the emulsion decreases, and a minimum viscosity is observed at the optimum formulation, irrespective of the formulation variable (e.g., EACN, salinity, nature of the surfactant; Salager, Miñana-Pérez, et al., 1983).

In Figure 8, we present additional examples of high-performance systems with low surfactant concentration, where the minimum interfacial tension can be used

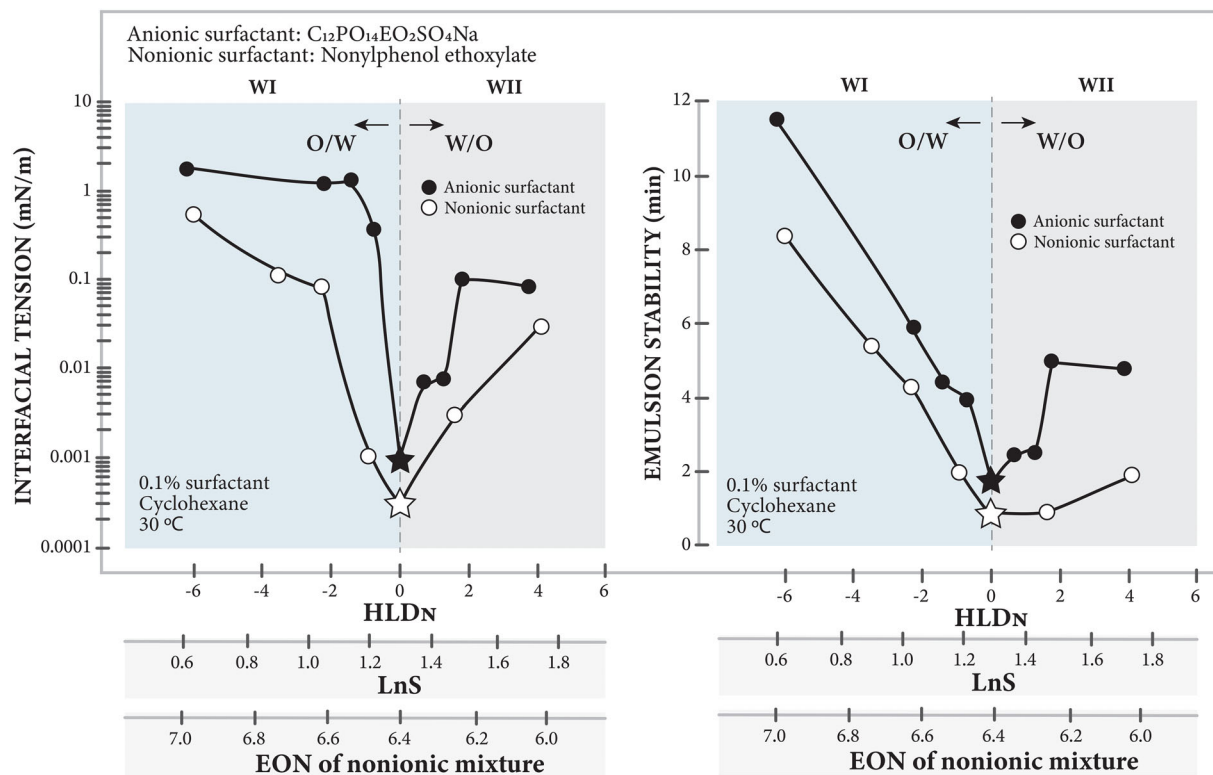


**FIGURE 8** Left: Interfacial tension minimum found at the optimum formulation of the anionic or nonionic surfactant/cyclohexane/brine system at 0.1 wt% surfactant when measured with the spinning drop apparatus.  $T = 30^{\circ}\text{C}$ . Right: Emulsion stability of the system measured as the time required for 50% of the volume of the aqueous phase after emulsification with an ultraturax apparatus for 30 s.

to determine the optimum formulation, as well as the minimum in emulsion stability (Marquez, Forgiarini, Fernández, et al., 2018). It is evident that in this case, a cyclohexane/brine system with either an extended anionic surfactant or an ethoxylated nonionic surfactant can achieve a very low interfacial tension at a low surfactant concentration of 0.1 wt%. It is crucial to highlight that the significant decrease in interfacial tension that occurs at the optimum formulation can be on the order of three orders of magnitude in this system with a high-performance surfactant, while the determination of the minimum by emulsion stability requires more precision. Emulsion stability can be very low around the optimum formulation and thus, the differences can be within the margin of error of the measurement and finding the exact point of the optimum can be challenging.

### Electrical conductivity of the emulsion

The electrical conductivity of the emulsified SOW system presents a change at the optimum formulation. In the most simple case, conductivity presents low values when W/O emulsions are formed (in the order of  $\mu\text{S}/\text{m}$  at  $\text{HLD} > 0$ ) and high values when O/W emulsions are obtained (in the order of  $\text{mS}/\text{m}$  at  $\text{HLD} < 0$ ) (Salager et al., 1982). Several theoretical equations have been developed to predict the electrical conductivity of two and

three-phase systems, given specific volume fractions and conductivities of the phases (Lee et al., 2003; Lee & Lim, 2005). However, it is currently not possible to use electrical measurements alone as a universal method for determining the morphology of the dispersed phases. This is because the conductivity depends largely on the conductivity of the external phase, and multiple morphologies may exhibit similar electrical conductivities. Therefore, it is necessary to use additional experimental methods in order to identify the morphologies that may be present in a system (Allouche et al., 2004; Johnson et al., 1994; Smith et al., 1994; Smith & Lim, 2000). Phase inversion may coincide with the minimum interfacial tension in the WIII zone in some cases, although this may not always be the case, even if the samples are pre-equilibrated and at  $\text{WOR} = 1$ . In Figure 9 it can be observed that the minimum of stability does not match exactly with the inversion indicated by the conductivity of the emulsion. Factors such as salinity, temperature, or pH could be at the origin of this delay (Salager et al., 1982), and will be discussed in a follow-up publication.

### Oscillating spinning drop interfacial rheometer

The OSDIR is a technique proposed by Slattery et al. (1980) (Slattery et al., 1980) and experimentally

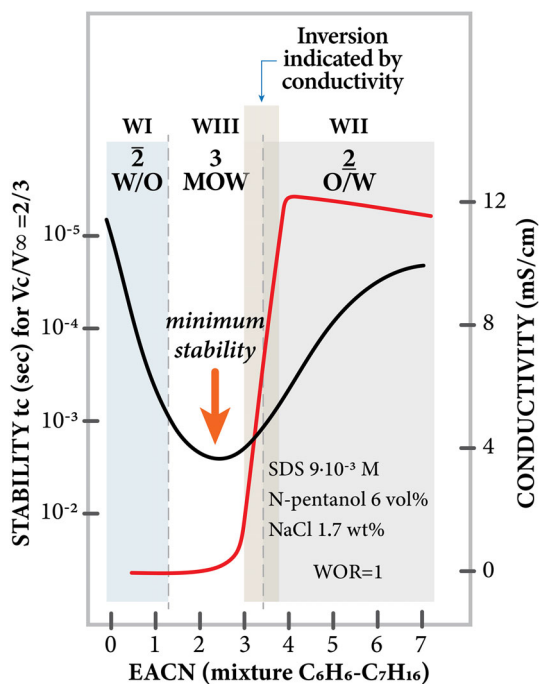


**FIGURE 9** Inversion point measured with conductivity in an emulsified SDS/n-pentanol/C<sub>6</sub>H<sub>6</sub>–C<sub>7</sub>H<sub>16</sub>/brine system and the corresponding emulsion stability. In some complex cases the conductivity of the emulsion might not coincide exactly with the minimum stability, the advantage is that conductivity can be measured in a short time and a continuous way with the so-called dynamic phase inversion method. Source: Adapted from Salager et al. (1982).

developed recently (Zamora et al., 2018), which operates with a principle similar to the spinning drop tensiometer, in this case, with an oscillating rotational speed. It is employed to measure interfacial dilational modulus of SOW systems, and it is particularly useful to measure the interfacial rheology modulus of systems at or near the optimum formulation (HLD = 0) (Figure 10). The dilational modulus, denoted as  $E$ , obtained with the OSDIR is equivalent to the Young modulus, which in a two-dimensional context, includes both compression and shear contributions (Zamora et al., 2018).

The OSDIR requires the appropriate selection of droplet volume, rotational speed, and oscillation amplitude to perform a precise measurement within a reasonable timeframe (Marquez, Bullon, Forgiarini, & Salager, 2021). This is particularly significant when dealing with systems that require long equilibration times, such as those containing high molecular weight or polymeric surfactants, which is the case in petroleum dewatering, typically associated with low interfacial tension (Marquez, Meza, Alvarado, Bullón, et al., 2021). The interfacial rheological measurement has been proven to be related to emulsion stability at the optimum formulation. In this case, the oscillation frequency ( $\omega$ ) can be set at 0.1 Hz to match the characteristic time scale of the phenomenon of emulsion breaking (Marquez, Forgiarini, Langevin, & Salager, 2018). In

contrast, a frequency sweep can be performed from  $\omega = 0.015$  to 0.25 Hz for a broader study of the system response to a frequency change.

The interfacial dilational modulus ( $E$ ) can be expressed by equation (Equation 9; Zamora et al., 2018):

$$E = A_0 \frac{\Delta\gamma}{\Delta A} \quad (9)$$

where  $\Delta\gamma$  represents the change in the interfacial tension,  $\Delta A$  is the variation in the drop area, and  $A_0$  is the initial interfacial area of the drop.

The measurements with the OSDIR have shown systematically that at HLD = 0, very low values of the dilational moduli and interfacial viscosity are attained, and thus, the optimum formulation can be identified (Marquez, Forgiarini, Fernández, et al., 2018). This is particularly important because it explains the very deep minimum in emulsion stability at optimum formulation (Marquez, Forgiarini, et al., 2019). We have identified a connection with interfacial rheology, specifically in cases in which low tension and Gibbs-Marangoni effects become negligible (Marquez, Forgiarini, Fernández, et al., 2018; Marquez, Forgiarini, Langevin, & Salager, 2018). In the past, the relationship between interfacial rheology and thin film stability has been extensively studied (Maru & Wasan, 1979; Tambe et al., 1995; Tambe & Sharma, 1991; Wasan et al., 1979; Wasan & Mohan, 1977). However, our recent research on the influence of formulation on interfacial rheology has definitively demonstrated that the moduli are extremely low at optimum conditions, which explains the strong coalescence and resulting low stability of the emulsion at this point (Marquez, Forgiarini, Fernández, et al., 2018; Marquez, Forgiarini, Langevin, & Salager, 2018). This occurs probably because the diffusional mass transfer is very fast at HLD<sub>N</sub> = 0 (Marquez, Antón, et al., 2019; Marquez, Forgiarini, et al., 2019; Marquez, Meza, Alvarado, Bullón, et al., 2021).

In this case, Figure 10 right panel presents the stability of the emulsion, measured as the separation of the aqueous or oil phase over time. It can be observed that outside the WIII zone, highly stable emulsions are achieved, and the dilational modulus is at least an order of magnitude higher than close to the optimum formulation. It can be said in different words that at the optimum, the interfacial modulus is extremely low, and emulsion stability decreases by three orders of magnitude when compared to emulsions outside the optimum formulation. This is significant for tailoring products where emulsion stability is a required property, such as in cosmetic emulsions or paints. Conversely, for systems for applications such as enhanced oil recovery or crude oil emulsion breaking, it is crucial to work near or at the optimum formulation, where a very low dilational elasticity and emulsion stability are attained.

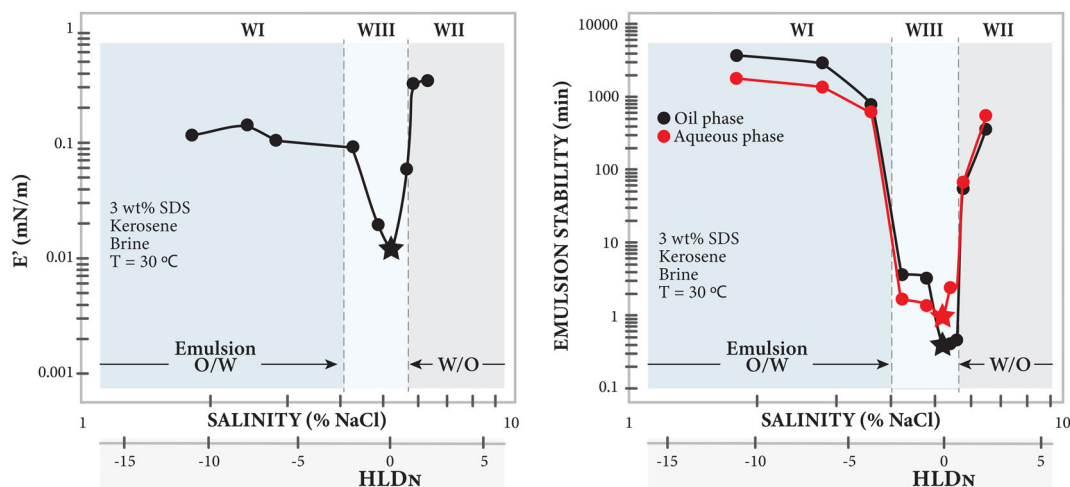


**FIGURE 10** Left: Interfacial dilatational modulus minimum found at the optimum formulation (5.2 wt% NaCl) when measured with the OSDIR. Right: Minimum emulsion stability measured with the volume separated of the phases (water or oil) after emulsification in a formulation scan in an SDS/Kerosene/Brine system at 3 wt% surfactant and 3 wt.% n-pentanol,  $T = 30^\circ\text{C}$ , Frequency = 0.1 Hz.

## COMPLEMENTARY TECHNIQUES THAT ALLOW UNDERSTANDING OF SOME STRUCTURAL FEATURES OF THE SOW SYSTEM AROUND THE OPTIMUM

Complementary techniques, such as light scattering methods, are increasingly being used to understand some structural features of SOW systems around the optimum formulation. These methods, which include DLS, small angle x-ray scattering (SAXS), and small angle neutron scattering (SANS), provide valuable insights into the size, shape, and morphology of these systems. On the other hand, NMR, x-ray micro-computed tomography (micro-CT), and DSC allow understanding changes in a formulation scan, such as identifying the zone around the optimum. However, their use in precisely determining the optimum formulation is limited. This is because the optimum formulation is a specific point, and while these techniques can help understand the region around the optimum, pinpointing its exact location can be challenging.

### Light scattering methods

Scattering techniques, such as light scattering (DLS), x-ray (SAXS), or neutron (SANS), have been used to obtain quantitative information regarding the size, shape, and morphology of microemulsions. These techniques operate by directing a beam of radiation onto the sample and measuring the intensity and angle of the scattered beam. The scattering phenomenon arises from the interaction of the radiation with regions of varying refractive index (light scattering), electron density (x-ray scattering), or nuclear composition (neutron scattering).

### Dynamic light scattering

DLS is a technique that can be used to analyze the size of structures near the optimum formation in a SOW system. It achieves this by determining the hydrodynamic radius, which can be extracted from measurements of the diffusion constants of the diluted dispersed phase (droplets) undergoing Brownian motion. DLS is advantageous as it utilizes simple equipment and requires short experimental times (Lemyre et al., 2010; Silva et al., 2007), although the interpretation of the data can be complex. The dynamics of microemulsions can be studied using a DLS setup by passing a laser beam through the phase of interest. The fluctuations in the intensity of the scattered light are collected as a function of time  $G_2(q, t)$ , and from the measured fluctuations the autocorrelation function of the intensity can be derived using the Siegert relation (Equation 10; Eyssautier et al., 2012):

$$G_2(q, t) = \alpha + \beta g_1^2(q, t), \quad (10)$$

in which case  $\alpha$  and  $\beta$  are a baseline and the coherence factor,  $q (= 4\pi n \sin(\theta/2)/\lambda_0)$  and  $t$  represent the scattering vector and time,  $n$  and  $\lambda_0$  are the refractive index of the medium and the radiation wavelength in vacuum.

For monodispersed systems, the dynamic behavior can be described using a normalized field autocorrelation function  $g_1(q, t)$ , which is expressed as a single exponential decay (Equation 11)

$$g_1(q, t) = \exp(-\Gamma t). \quad (11)$$

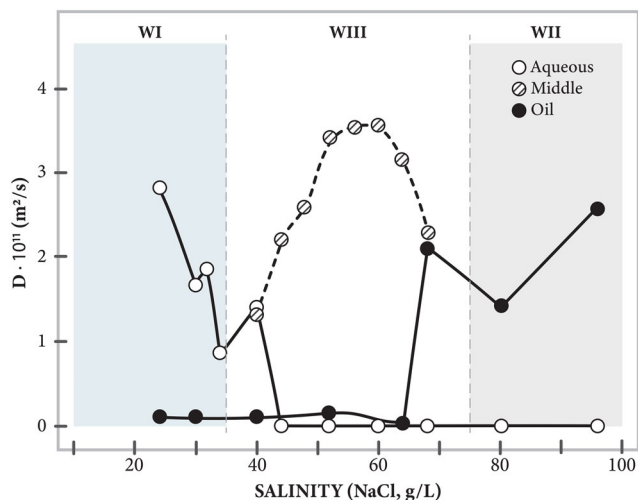


**FIGURE 11** Diffusion coefficients of microemulsions formed with sodium dodecyl benzenesulfonate, isobutanol, brine, and decane at different salinities reach a maximum around the optimum salinity 52 g/L. Source: Adapted from Fukumoto et al. (2016).

The diffusion coefficient of the particles is defined as  $D = \Gamma/q^2$ , where  $\Gamma$  is the exponential decay rate and  $q$  is the scattering vector, and in the case of hard spheres dispersed in solution, with no interactions under the influence of Brownian motion, the hydrodynamic radius  $R_H$  of a sphere given by the Stokes-Einstein equation as (Equation 12):

$$D = \kappa T / 6\pi\nu_0 R_H, \quad (12)$$

in which  $\kappa$ ,  $T$ , and  $\nu_0$  are the Boltzmann constant, temperature, and viscosity of the solvent.

Fukumoto et al. (2016) investigated the dynamics of microemulsions formed with sodium dodecyl benzenesulfonate, isobutanol, brine, and decane, at different salinities through DLS. To that end, the authors calculated the hydrodynamic radius for Winsor I and Winsor II systems formed by swollen micelles. However, for Winsor III systems, this parameter is not suitable. The authors calculated the diffusion coefficient  $D$  for all phases obtained by performing a formulation scan of the SDBS/decane/isobutanol/brine system from 3 to 8 wt% NaCl, noting that the calculated  $D$  of a Winsor III system does not represent the diffusivity of the components in the middle phase, but corresponds to the characteristic time of the dynamics. By plotting  $D$  of microemulsion aqueous, middle, and oil phases against salinity, the authors found that the value of  $D$  in the middle phase reached a maximum value near the optimum salinity, 52 g/L, (Figure 11) and attributed this behavior to topological changes and the smaller domain size. The results obtained in this research for  $D$  of the middle phases were consistent with those reported in the literature (Shukla et al., 2004) and proved the efficacy of the DLS technique in quantifying the optimum salinity.

There are some limitations of the technique in practice. DLS assumes that the system is monodisperse and there is low sensitivity to large particles. Furthermore, samples with high viscosity may not provide reliable results, and opaque systems have limitations, even if a backscattering configuration is used.

## Small angle scattering

In small-angle x-ray scattering (SAXS), the scattering profile obtained at low angles is analyzed by fitting it to appropriate models. This allows for the extraction of information about the shape, size, and nanostructure of scattering elements present in microemulsions (Berti & Palazzo, 2014). To investigate microemulsion structures on the desired scale (greater than 10 nm), scattering angles smaller than  $1^\circ$  are typically used. SAXS is employed in determining the shape and size of microemulsion droplets by leveraging the disparity in the x-ray scattering abilities of the oil and water phases. This characteristic is frequently applied to estimate the radius of the confined phase in oil-in-water (O/W) or water-in-oil (W/O) swollen micelles (Blochowicz et al., 2007; Roshan Deen & Pedersen, 2008).

Using several experimental techniques, Fukumoto et al. (2016) examined the physical properties and morphologies of microemulsions formed with sodium dodecyl benzenesulfonate, isobutanol, brine, and decane. Among those techniques, SAXS proved to be effective in the characterization of microemulsion systems morphology and composition. The SAXS spectra for the microemulsions at different brine concentrations is shown in Figure 12. A single broad peak was identified for the scattering curves of microemulsions at 40, 52, and 64 g/L salinities, which is characteristic of bicontinuous microemulsions (Chen et al., 1990), while for the O/W at 30 g/L and W/O at 80 g/L Winsor I and Winsor II systems, no characteristic peak was observed. The solid line for the scattered intensity  $I(q)$  of the Winsor I system at 30 g/L (shown in Figure 12) was calculated by the authors from the Guinier approximation (van Blaaderen & Vrij, 1992).

The authors used the Teubner and Stray (T-S) model to fit the scattered intensity  $I(q)$  for the bicontinuous microemulsions at 30, 40, 52, and 64 g/L (Teubner & Strey, 1987), and thus obtained the physical parameters for the domain size  $d$ , and the correlation length  $\xi$ , which were in the same range as those reported in the literature (Chen et al., 1991; Teubner & Strey, 1987).

On the other hand, for the 80 g/L microemulsion, the Guinier fitting did not agree with the measurements since there was no plateau in the spectra, and therefore no line was drawn. As shown in Figure 12, good agreement between the SAXS measurements and the fitted line from the model is found in the  $q$  range below

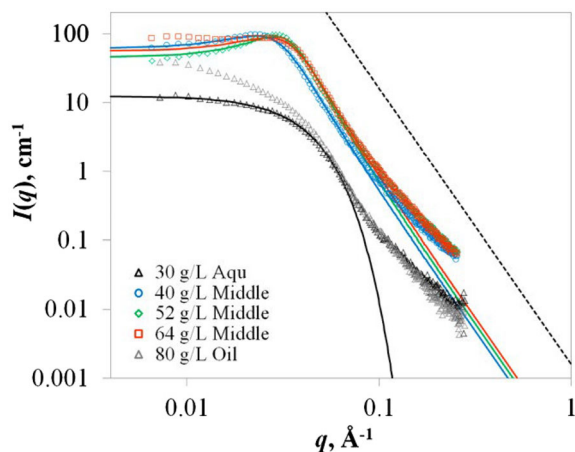


**FIGURE 12** SAXS spectra of microemulsions formed with sodium dodecyl benzenesulfonate, isobutanol, brine, and decane at different salinities. Winsor I system at 30 g/L, Winsor III at 40, 52 and 64 g/L, and Winsor II at 80 g/L. The SAXS measurements were fitted with the Teubner and Stray (T-S) model or the Guinier equation (solid lines). The dashed line represents the power of law of  $q^{-4}$ . Source: Reproduced from Fukumoto et al. (2016).

$0.07 \text{ \AA}^{-1}$ . Remarkably, for the bicontinuous microemulsion systems (Winsor III), the domain size  $d$  showed a minimum, and the correlation length  $\xi$  a maximum at the optimum formulation, 52 g/L. SAXS seems a prospective technique that proves to be effective for the optimum formulation and surfactant parameter (SCP) quantification in the HLD equation, although access to a SAXS system is required. Measurements can be lengthy and subjected to certain precautions, as indicated in Table 1.

Other techniques, such as SANS allows to gain information on the size and shape of the structures formed in the surfactant-rich phase (Gradzielski et al., 2021; Hellweg, 2009; Prévost et al., 2017). However, systems with low contrast could potentially limit the amount of information obtained from the scattering data. Moreover, the interpretation of SANS data can be complex and may require a deep understanding of both the experimental technique and the system being studied. The complexity increases in practical cases, making the observation more challenging and the measurement requires significant resources, including neutron sources. This is probably why there are only a handful of works where formulation scans have been performed with SANS to gain information on the structure of the microemulsion and not to identify the optimum formulation (Choi et al., 2002; Gradzielski et al., 2021).

## Nuclear magnetic resonance

NMR has been extensively used to provide structural information on microemulsion systems by measuring

the self-diffusion coefficients of the different components of such complex mixtures (Furó, 2005; Lindman et al., 2020), including the surfactant rich phases at equilibrium around the optimum formulation.

This technique, regarded as non-invasive, versatile, precise, and fast, allows to differentiate between discontinuous (called type WI and WII) and bicontinuous (type WIII) microemulsions, as well as determining whether a swollen micellar system around the optimum is normal (HLD < 0) or inverse cases (HLD > 0) type.

This is possible because the self-diffusion coefficients of the oil- or water-continuous phase in swollen micellar system are similar to those of the bulk liquid. Simultaneous high diffusion coefficients of both component solvents indicate the presence of bicontinuous structures at HLD = 0, and a significant change in the diffusion properties of one solvent indicates the transition from bicontinuous to swollen micellar systems at a distance from the optimum. Two main NMR experiments are used: relaxation and self-diffusion studies. Of these two, self-diffusion studies have been extensively used to characterize microemulsion systems (Lif et al., 2009; Lindman et al., 1980), even if there is no really an interface but a dispersion of aggregates in a single phase. On the other hand, relaxation studies have fairly been conducted on microemulsions due to the low sensitivity of this technique to inter-object interactions.

In a recent study, Herrera et al. (2021) applied an innovative approach to extract compositions and follow the kinetics of microemulsion formation (Herrera et al., 2021). The authors used a high-resolution  $T_1$ -weighted relaxometry imaging NMR system to access 1D-composition profiles of cosurfactant, oil and brine in Winsor I, and II swollen micellar systems and Winsor III bicontinuous microemulsions. The results obtained from this technique are comparable to those reported in the literature (Bellocq et al., 1980; Pouchelon et al., 1981). Figure 13 depicts the NMR profiles obtained for SDS/n-butanol/NaCl brine/Toluene systems at different salinities, as a function of the height of the testing tube, during each formulation step.

This technique could be employed to determine the optimum formulation based on the quantification of NMR profiles of the different phases present in the microemulsion systems. This method presents several advantages, such as giving access simultaneously to oil, brine, and co-surfactant compositions; it is non-destructive, relatively fast, reproducible, and can be employed to quantify opaque/dark systems. However, one of the significant drawbacks is the limited quantification for components at concentrations below 4% vol % and requires a contrast in  $T_1$ -relaxation time and/or hydrogen index between each system component (Herrera et al., 2021). While NMR requires specialized

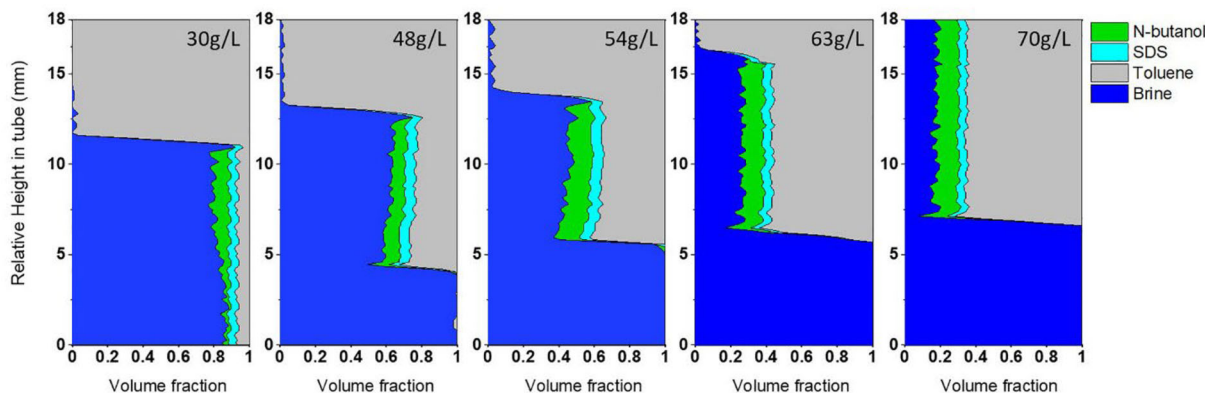


**FIGURE 13** Volume fractions of each component at different salinities, for Winsor I, Winsor II and Winsor III SDS/n-butanol/NaCl brine/Toluene systems obtained from NMR profiles. T = 25°C. Source: Reproduced from Herrera et al. (2021).

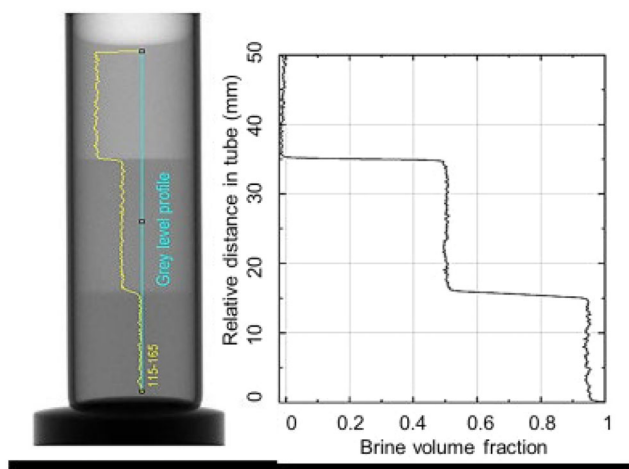


**FIGURE 14** Micro-CT radiography of an equilibrated SDS/n-butanol/NaCl brine / Toluene microemulsion at optimal salinity (left). T = 25°C. Conversion of gray profiles from the radiography to brine volume fractions along the testing tube. Source: Reproduced from Herrera et al. (2021).

equipment and expertise, the data it provides often justifies the associated time and cost in the case of very complex phases, such as opaque ones that are difficult to measure with other techniques.

### X-ray micro-computed tomography

The micro-CT method is based on transmitting x-ray radiation through a sample. Radiographies of the samples are acquired over time and displayed in levels of grays (Unsal et al., 2019; Figure 14). The absorbance of the sample is dependent on the attenuation coefficient,  $\mu_i$ , volume fraction,  $\phi_i$ , of each component  $i$  in the system, and the thickness of the transmitting medium,  $x$ , and varies according to the Beer–Lambert law.

The brine distribution can be easily extracted from this technique due to a contrast in attenuation coefficients of water and the other components of the system. The volume fraction of the brine along the testing tube can be calculated from Equation 13, with  $X_{brine}(h)$ , the volume fraction of brine at height  $h$  of the testing tube,  $I_{oil}$  and  $I_{brine}$  the reference intensities for oil and brine (Herrera et al., 2022).

$$X_{brine}(h) = \frac{\ln(I_{oil}) - \ln(I_{sample}(h))}{\ln(I_{oil}) - \ln(I_{brine})} \quad (13)$$

One of the major limitations of this technique is that no significant contrast is observed for the reference surfactant-water system and water alone, limiting the detection of the surfactant in the different phases. However, the micro-CT is substantially reliable in quantifying the relative distance in the tube of the different phases present in a three-phase system, therefore proving useful to measure the volume fraction of each component.

The results obtained by x-ray micro-CT for microemulsion systems have been compared to other techniques, such as NMR, and good agreement is found in terms of volume fraction for the different phases. Although, the results obtained from both techniques exhibit disparities for systems far from the optimal salinity (1 to 7 vol%).

In a recent article, Borji et al. (2022) showed that the classical visual phase-behavior tests might be misleading since coloring of the aqueous-phase can occur due to even minor contamination of water with crude oil, which makes the water phase optically indistinguishable from the oil phase (Borji et al., 2022). In that sense, micro-CT scanning is objective and quantitative regarding phase composition and can provide information about the optimum concentration in agreement with classical experiments.

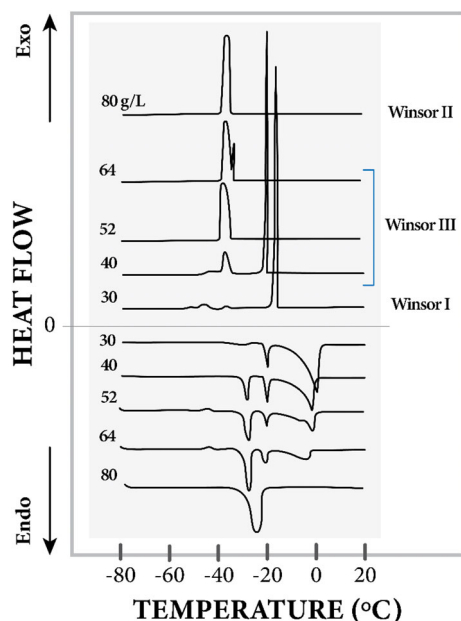


**FIGURE 15** Heat flow profiles of microemulsions formed with sodium dodecyl benzenesulfonate, isobutanol, brine, and decane at different salinities. Winsor I system at 30 g/L, Winsor III at 40, 52, and 64 g/L, and Winsor II at 80 g/L. Source: Reproduced from Fukumoto et al. (2016).

## Differential scanning calorimetry

The DSC has been used to characterize the morphology of emulsions (Clausse et al., 2005). In a classical DSC experiment, regular heating and cooling cycles are applied to an emulsion at temperatures that are within the freezing and melting points of the dispersed droplets.

Dalmazzone et al. (2009) used DSC to characterize the phase behavior of emulsified systems, and were able to deduce relevant information, such as type of emulsion, amount of water, presence of solute, stability, and droplet size from the thermograms (Dalmazzone et al., 2009; Fukumoto et al., 2018). Studies have demonstrated a correlation between the water morphology and the temperature at which microemulsions crystallize, as the likelihood of ice nucleation is directly proportional to the volume of water. Reports show that the smaller the water volume, the lower the freezing temperature. Fukumoto et al. (2016) investigated the physical properties and morphologies of microemulsions formed with sodium dodecyl benzenesulfonate, isobutanol, brine, and decane, through DSC. The heat flow profiles of the microemulsions at different salinities are shown in Figure 15.

Three characteristic behaviors are observed for the microemulsion systems during the cooling process (Figure 12). The heat flow profiles for the systems

containing salinities of 30 and 40 g/L display two sharp positive peaks around  $-20^{\circ}\text{C}$ . This indicates the presence of water in a  $\text{mm}^3$  volume scale and is expected for the 30 g/L system since the microemulsion is Winsor I type, in which eventually oil swollen micellar aggregates are dispersed in a continuous water phase. For the 40 g/L system, which contains a bicontinuous middle phase structure (Winsor III), it might be thought that the size of the water channels in the microemulsion are so large that there is no peak shift despite the bicontinuous structure formation, but that was not the case.

Instead, a phase separation of water and oil domains surrounded by a continuous surfactant film coating occurred as the authors confirmed it. This phase separation did not occur for salinities of 52 and 64 g/L. Second peaks were also observed for these two systems around  $-35^{\circ}\text{C}$ , corresponding to decane crystallization. In addition, third peaks were detected between  $-45$  and  $-40^{\circ}\text{C}$  and attributed to NaCl crystallization. The microemulsion at optimum salinity (52 g/L) exhibited only one crystallization peak, supporting that water and oil crystallization are happening together.

A small sharp peak was observed at  $-32^{\circ}\text{C}$  for the 64 g/L microemulsion, following the characteristic peak for decane crystallization, indicating the presence of water in a volumetric scale of  $\mu\text{m}^3$  in the bicontinuous middle phase. For the Winsor II system, 80 g/L salinity, a single peak at  $-35^{\circ}\text{C}$ , was shown, attributed to the decane crystallization. Since this system is an oil solution of eventually swollen inverse micelles, it is expected that the surrounding decane induces the crystallization of water droplets and therefore, the single peak corresponds to the freezing of water and decane simultaneously.

## COMPLEX CASES FOR THE DETERMINATION OF THE OPTIMUM FORMULATION

While the methods mentioned in the previous section may yield accurate results for preequilibrated systems before emulsification, inconsistencies can still be found if some surfactant/cosurfactant transfer between phases has to happen. In Figure 16 system, sec-butanol and surfactant are initially introduced in the oil phase, and the optimum formulation is at  $S^* = 0.45$  wt% from the phase behavior in an equilibrated system after 24 h of contact (Salager, Moreno, et al., 2002). The emulsion inversion also happens at the same formulation without any contact time, that is, the equilibration can occur instantly at or close to the optimum formulation in the WIII phase behavior ( $0.45 < S < 0.50$ ). However, slightly away from optimum (e.g.,  $S < 0.40$ ), the contact time required to produce an apparent pseudo-equilibration ( $t_{APE}$ ) is nonzero and it



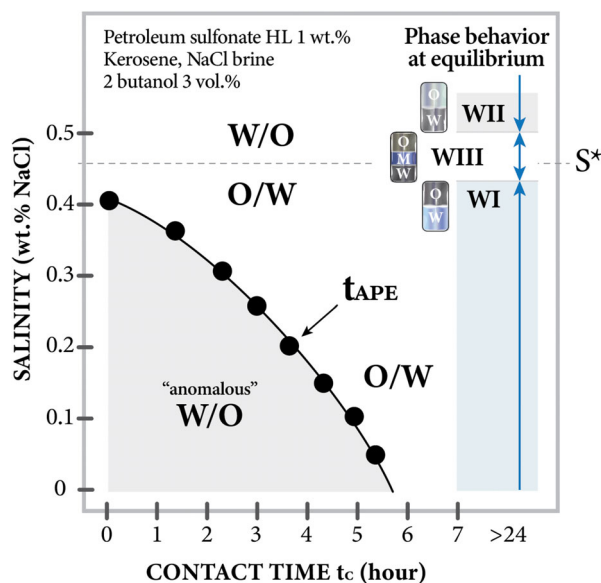


**FIGURE 16** Change in preequilibration time when a system is nearing optimum formulation. The salinity is shown as a function of the contact time ( $t_c$ ) to attain a normal morphology of the emulsion. Near HLD = 0 at 0.45% NaCl the preequilibration time is effectively almost zero hours. *Source:* Adapted from Salager, Moreno, et al. (2002).

increases as the formulation departs from optimum. This is consistent with an analysis suggesting that the pseudo-equilibration time is very short probably due to an increased surfactant mass transfer in the presence of the middle phase with a bicontinuous structure (Fillous, Cardenas, et al., 1999). It means that if the surfactant/cosurfactant is introduced in the water phase, a similar far from optimum zone with a long preequilibration will also happen above  $S = 5$  wt%. Consequently, it can be said that the determination of the zone with a zero  $t_{APE}$  may be a way to determine the optimum formulation. Nevertheless, the corresponding experiences are extremely long and the methods are not attractive, even with simplified cases (Cardenas et al., 2001; Fillous, Cárdenas, et al., 1999).

### The effect of oil viscosity on the formulation versus composition map

The coincidence between emulsion phase inversion and the minimum interfacial tension in the WIII zone occurs when the formulation-composition WOR diagram has an inversion line and a three-phase horizontal zone. However, this may not always be the case, as the inversion zone is often tilted (as already indicated in Figure 3) in one direction or the other (Antón et al., 1986), and the HLD formulation and system complexity appear to be the main factors influencing this approximative coincidence. For example, a decrease in

surfactant concentration can result in the B<sup>-</sup> zone becoming larger, causing the transitional inversion line to become very slanted, as depicted in Figure 17 for a relatively simple SOW system. On the other hand, an increase in the oil phase's viscosity can also lead to the transitional inversion line becoming slanted or disappearing at high viscosities (Figure 18). These types of systems, which are characterized by low surfactant concentration of less than 1 wt% and high viscosity, are often found in applications such as crude oil dewatering and cosmetics. Therefore, it is important to study specific systems in detail, as general trends have not yet been fully understood.

### Electrical conductivity measured in emulsified preequilibrated systems can present coincidence (or not) with the WIII zone

Understanding the phenomena that occur outside the transitional inversion driven by changes such as temperature, salinity, and other factors, unrelated to curvature changes, is crucial. For example, when the water-oil ratio (WOR) is different or far away from unity.

An example of this complex behavior is presented in Figure 19, where previously preequilibrated systems that are emulsified present changes in conductivity according to the water-to-oil relationship (WOR). These figures indicate that, for the SDS/kerosene/brine/n-pentanol system, the emulsion conductivity coincides with the Winsor III zone exactly at WOR = 1 ( $fw = 0.5$ ), but outside this zone, the change in emulsion conductivity occurs not exactly at the middle of the Winsor III zone or even outside. Therefore, it is crucial to determine the circumstances under which emulsion inversion may be influenced by factors such as temperature, salinity, and others. In particular, the speed at which these changes occur can significantly affect the process, potentially leading to substantial hysteresis or delays. To avoid these issues, a comprehensive assessment of the impact of variables such as surfactant concentration, WOR, oil viscosity, and others on the emulsion inversion process is required. These aspects are not obvious and will be dealt with in a future publication.

### Final comments on methods to detect optimum formulation according to accuracy and application

After Winsor's work 70 years ago, it was clear that the way to determine the "optimum" formulation to produce a three-phase behavior occurrence (as in a Winsor III diagram) was through a formulation scan. Winsor and

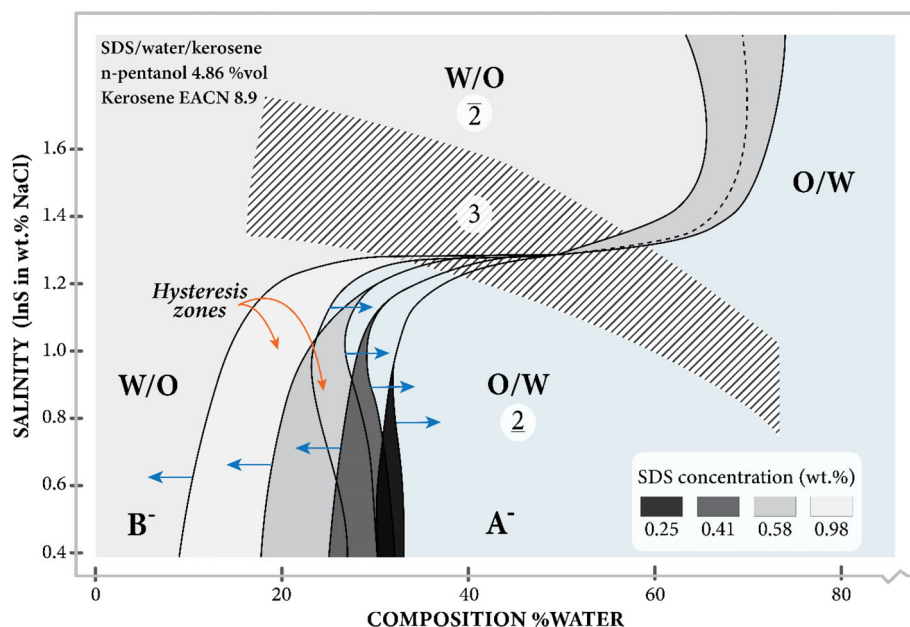


**FIGURE 17** Variation of the inversion locus when surfactant concentration and WOR are changed. Source: Adapted from Silva et al. (1998).

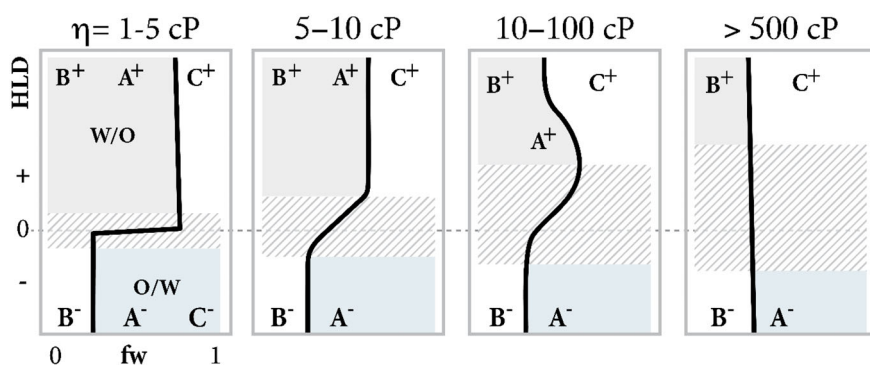


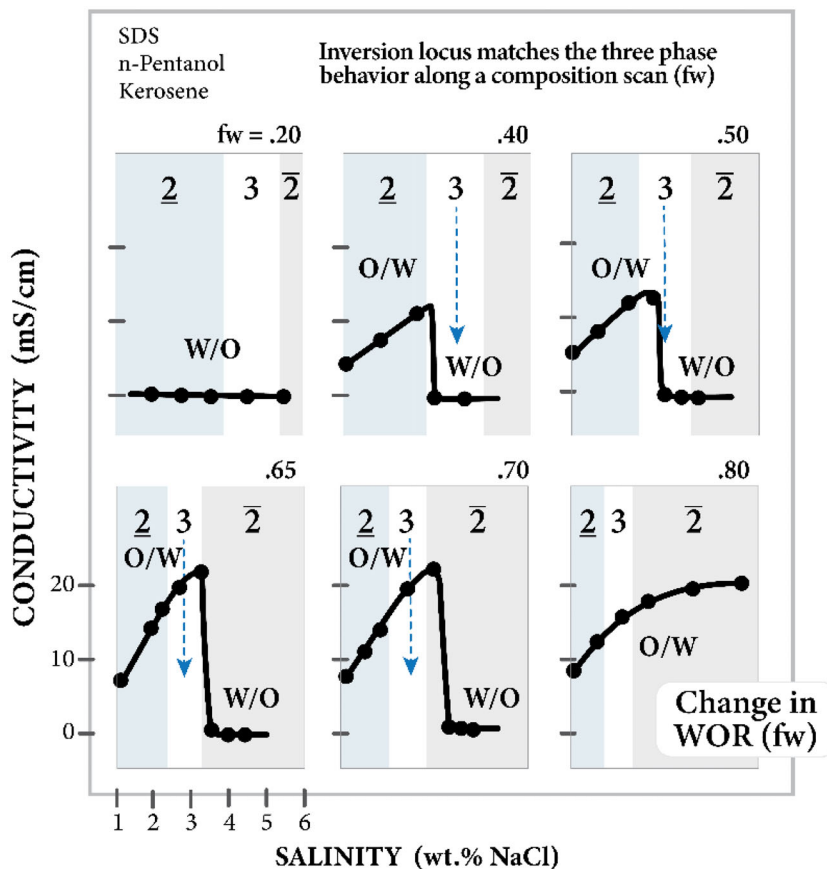
**FIGURE 18** Variation of the inversion locus in a formulation versus composition map in which the inversion line changes with viscosity making the transitional line almost disappear. SDS 0.02 M, n-Pentanol 4.7 vol%, kerosene-lube oil mixture, brine (NaCl). Source: Adapted from Salager et al. (1990), Salager, Miñana-Perez, et al., (1983).

other researchers pointed out that certain intervals can be established for the three-phase systems, in which very low interfacial tensions and a high solubilization of oil and water might occur, or poor solubilization with higher interfacial tensions (Barakat et al., 1982, 1983). In the first case, the accuracy to determine the optimum was good and the data collected from the WI and WII “lateral” systems could be extrapolated to approximately guess the optimum, for instance, by measuring the volume of the phases in the WIII range, that is, by looking at the O and W equal solubilization in the middle phase. This was often accurate for systems containing ionic surfactants and short alkanes. On the other hand, for systems containing large volumes of WIII phase, systems containing nonionic surfactants, and long-chain alkanes, it was not easy to measure the optimum by a simple linear relationship between two formulation variables.

There was also some discrepancy between the different types of detection of the optimum detection in the scan, as the center of three phase behavior, the minimum tension, the minimum emulsion

stability, or the conductivity variation. Some discrepancies also arise for the accurate detection of the optimum, with different authors considering different parameters. The inaccuracy could also come from the fact that the “middle” of a three-phase behavior range is not clear with a logarithmic scale used for a salinity formulation scan or for the emulsion electrical conductivity. The accuracy is also altered by the system performance, that is, the intensity of variation close to optimum. In other words, it can be said that with a very narrow three-phase range that is associated with a very deep minimum tension, the determination of the exact optimum position could be easy, even if the actual tension measurement is not very easy. On the contrary, with a very wide three-phase behavior range, the determination of the optimum somewhere in the three-phase range could be inaccurate, and more measurements of the tensions are required, with an increased experimental cost (Barakat et al., 1982; Klaus et al., 1983; Salager et al., 2017) but with improved data on the system robustness.

**FIGURE 19** Complex cases in which the conductivity changes inside or outside the Winsor III behavior zone. It can be seen that only at WOR exactly equal to 1 ( $fw = 0.5$ ) the change in conductivity and Winsor III zone perfectly coincide. Source: Adapted from Salager, Miñana-Pérez, et al. (1983).



Equilibration of the SOW system before the measurement of a property is theoretically important, but in practice, the experiment time must be as short as possible, thus, some compromise is needed. If the equilibration at the interface is far from being reached, inaccuracy could happen with respect to the theoretical expectation concerning the interfacial adsorption, the interfacial tension, the mass transfer, the emulsion type and inversion, and so forth. If the process used is dynamic, like a continuous variation in formulation as changing temperature (used mainly for theoretical research) or adding a component, or producing a composition variation like dilution, delays in pseudo-equilibration at interface through some mass transfer can result in hysteresis and sometimes wrong interpretations.

On the contrary, it can be said that experiments performed with original systems very close to the optimum formulation are very quickly equilibrated, that is, a few seconds or minutes. Thus, the body of knowledge and know-how developed around formulation indicates that the optimum formulation determination process should be performed in two steps. This first one is a very quick and quite inaccurate trial (with only a few experiments) to very approximately determine the optimum formulation zone, and then a second approach with good accuracy in a narrow range very close to optimum.

However, it could be insufficient in some cases, as in the injection of an EOR liquid stream in a petroleum reservoir with very different temperature, pressure, and salinity values, as well as a quite different water/oil ratio and thus partitioning of mixtures. Thus, the researchers and authors experience in the past half century is essential for the knowledge that has been brought to be available, although with some arbitrary or voluntary confusions, and that any new user of this knowledge must be able to see the trends and understand divulgation of the know-how by reading the literature wisely.

This remark is critical because it has been shown in different ways that the optimum found through a conductivity change or a three-phase behavior occurrence, or a minimum tension could be consistent only in some cases. For instance, only at a specific WOR, often close to unity, with a very strong discrepancy below or above it (Lemahieu et al., 2022; Marquez et al., 2003).

Consequently, it happens that it is of utmost importance that the application of the different techniques for the determination of the optimum formulation must be checked for their generalized validity if some of the formulation or composition variables are changed.

The last comment of this review article will be that this situation is too often occurring in the area of SOW systems, as mentioned in the preface of Milton Rosen applied book: *The basic principles involved in surfactant*

utilization are often obscured by the mathematics, and too far away from real-life applications (Rosen & Dahanayake, 2000).

## CONCLUSIONS AND PERSPECTIVES

The optimum formulation in SOW systems can be determined more or less accurately by using different techniques, among them phase behavior, interfacial tension, and interfacial dilational modulus of equilibrated systems, as well as emulsion properties like stability, conductivity, and viscosity. While these methods have been used to determine the optimum formulation (at HLD = 0), in some cases, there have been discrepancies in the detection of the optimum in the scan, such as the center of three-phase behavior and the minimum interfacial tension with the minimum emulsion stability, or the conductivity variation. The techniques used after the system has reached the equilibrium allow measuring the optimum accurately, while in the cases measured in emulsified systems, complex phenomena can occur outside the equilibrium. This has to do with the preequilibration of the SOW system before the measurement of a property, which is theoretically important, but in practice, the experiment time must be as short as possible for cost reasons. Thus, phenomena related to interfacial adsorption, mass transfer, the emulsion type and inversion can occur in these cases. These complex cases of emulsion inversion will be discussed in extension in a future publication.

Multiple complementary techniques can be used in determining some structural features in a SOW system formulation scan. Scattering techniques, which provide nanostructural information in ambient conditions, have been used in some examples to characterize various types of cases from single phase so-called swollen micelle systems WI or WII or bicontinuous microemulsions WIII type. SAXS has demonstrated effectiveness in identifying optimum salinity and providing insights into the structure of single phase microemulsion systems, while DLS has proven its value in studying the dynamics of the middle-phase so-called bicontinuous microemulsions. Although scattering techniques are excellent in extracting structural information, their main weakness is in the area of capturing information about dynamic processes at very short time scales, and thus to determine the optimum formulation understood as exactly the minimum tension occurrence. On the other hand, high-resolution T1-weighted relaxometry imaging NMR systems have shown promising results in studying the kinetics of microstructure formation, thus, identifying the composition of the phases, including the middle phase. Micro-CT has proven effective in quantifying the thickness of various phases present, despite the difficulty in detecting the surfactant in different phases. This method relies on high-tech equipment

and may not be applicable in all cases. Finally, DSC analysis has shown a correlation between the morphology of the phases and the temperature at which colloidal structures crystallize into a separated solid. This analytical technique is useful when precise temperature control and detailed analysis of phase transformations are necessary. As these methods develop further, they might be used more frequently, although their application is currently limited to specialized cases.

Different cases of so-called microemulsions continue to be the subject of academic and industrial research still with some semantics confusion (Salager et al., 2020; Salager, Graciaa, & Marquez, 2022; Salager, Marquez, Rondon, et al., 2023), extending beyond their initial recurring theme of enhanced oil recovery (EOR). They have become associated with the “optimum formulation” concept and are now being used in increasingly demanding applications that require more sustainable components and innovative formulations. The use of ionic liquids (Kunz et al., 2012), supercritical fluids like CO<sub>2</sub> (Eastoe et al., 2012), non-aqueous microemulsions (Bourrel & Schechter, 2010; Schubert et al., 1992), and other types of oil/water systems highlight the need to perform research on the application of the same techniques used for the typical SOW systems (Prévost et al., 2017; Vitale & Katz, 2003; Zemb et al., 2016). Systems consisting of oil and water solubilized as a homogeneous phase thanks to hydrotropes (i.e., short alcohols) are an example (Gradzielski et al., 2021; Kunz et al., 2016). Even if the structures are different from so-called bicontinuous microemulsions, interfacial tension presents also a minimum and conductivity, DLS, NMR, and SAXS are tools that allow understanding the solubilization phenomena.

In the context of formulation, the HLD concept will continue to play a pivotal role. The challenge of adapting the HLD equation to complex systems involving components such as two immiscible oils, ionic liquids, or supercritical fluids could lead to significant advancements in rational formulation. Additionally, the substitution of fossil-derived by biobased or biosurfactants will require a thorough determination of surfactant parameters for these new products that are becoming important in the market and in companies. There are almost no results on biobased or biosurfactants surfactant contribution parameter (SCP or PACN) within the HLD framework. In order to perform the task of characterizing all the surfactants that are entering into new lower carbon footprint products, revisiting the methods to determine the optimum formulation for complex systems is crucial.

## AUTHOR CONTRIBUTIONS

**Ronald Marquez:** Conceptualization, methodology, writing – original draft, writing – review and editing.  
**Jesús F. Ontiveros:** Conceptualization, methodology, writing – original draft, writing – review and editing.

**Nelson Barrios:** Methodology, writing – original draft, writing – review and editing. **Laura Tolosa:** Writing – review and editing, visualization. **Gerardo Palazzo:** Writing – review and editing. **Véronique Nardello-Rataj:** Writing – review and editing. **Jean Louis Salager:** Conceptualization, methodology, writing – original draft, writing – review and editing.

## ACKNOWLEDGMENTS

The authors would like to thank their colleagues and publication ex-coauthors from research centers in Venezuela, USA, and France for helpful and enlightening discussions related to the optimum formulation determination techniques. They are (in historical order): Robert Schechter and William Wade (USA), Raquel Antón, Johnny Bullón and Ana Forgiarini (Venezuela), Jean-Lachaise, Lionel Choplin, Dominique Langevin, Jean-Marie Aubry (France). The authors want to thank also all the PhD students and researchers from FIRP Laboratory (University of Los Andes), CISCO team (University of Lille), and CSGI team (University of Bari) that contributed to the body of knowledge on the subject.

## FUNDING INFORMATION

NC State University is acknowledged for the support given to two of the authors.

## CONFLICT OF INTEREST STATEMENT

The authors declare that they have no conflict of interest.

## ETHICS STATEMENT

No human or animal subjects were used in this research.


## ORCID

Ronald Marquez  <https://orcid.org/0000-0001-6003-7487>

Jesús F. Ontiveros  <https://orcid.org/0000-0001-8188-049X>

Nelson Barrios  <https://orcid.org/0000-0002-9932-9775>

Laura Tolosa  <https://orcid.org/0000-0002-9862-9733>

Gerardo Palazzo  <https://orcid.org/0000-0001-5504-2177>

Véronique Nardello-Rataj  <https://orcid.org/0000-0001-8065-997X>

Jean Louis Salager  <https://orcid.org/0000-0003-4495-7333>

## REFERENCES

- Acosta E. The HLD–NAC equation of state for microemulsions formulated with nonionic alcohol ethoxylate and alkylphenol ethoxylate surfactants. *Colloids Surf A Physicochem Eng Asp.* 2008;320:193–204. <https://doi.org/10.1016/j.colsurfa.2008.01.049>
- Acosta E, Yuan JS, Bhakta AS. The characteristic curvature of ionic surfactants. *J Surfactant Deterg.* 2008;11(2):145. <https://doi.org/10.1007/s11743-008-1065-7>

- Allouche J, Tyrode E, Sadtler V, Choplin L, Salager J-L. Simultaneous conductivity and viscosity measurements as a technique to track emulsion inversion by the phase-inversion-temperature method. *Langmuir.* 2004;20(6):2134–40. <https://doi.org/10.1021/la035334r>
- Al-Sabagh AM. The relevance HLB of surfactants on the stability of asphalt emulsion. *Colloids Surf A Physicochem Eng Asp.* 2002;204(1–3):73–83. [https://doi.org/10.1016/S0927-7757\(01\)01115-3](https://doi.org/10.1016/S0927-7757(01)01115-3)
- Antón RE, Castillo P, Salager J-L. Surfactant–oil–water systems near the affinity inversion. Part IV: emulsion inversion temperature. *J Dispers Sci Technol.* 1986;7(3):319. <https://doi.org/10.1080/01932698608943463>
- Antón RE, Salager J-L. Emulsion instability in the three-phase behavior region of surfactant–alcohol–oil–brine systems. *J Colloid Interface Sci.* 1986;111:54–9. [https://doi.org/10.1016/0021-9797\(86\)90006-8](https://doi.org/10.1016/0021-9797(86)90006-8)
- Aubry JM, Ontiveros JF, Salager J-L, Nardello-Rataj V. Use of the normalized hydrophilic-lipophilic-deviation (HLDN) equation for determining the equivalent alkane carbon number (EACN) of oils and the preferred alkane carbon number (PACN) of nonionic surfactants by the fish-tail method (FTM). *Adv Colloid Interf Sci.* 2020;276(220):102099. <https://doi.org/10.1016/j.cis.2019.102099>
- Bansal VK, Shah DO. *Microemulsions and tertiary oil recovery.* Microemulsions. New York, London: Academic Press; 1977. p. 149–73.
- Barakat Y, Fortney LN, Schechter RS, Wade WH, Yiv SH. Alpha-olefin sulfonates for enhanced oil recovery. *Proceedings of the 2nd European symposium enhanced oil recovery*, 11–20. 1982.
- Barakat Y, Fortney LN, Schechter RS, Wade WH, Graciaa A. Criteria for structuring surfactants to maximize solubilization of oil and water: II. Alkyl benzene sodium sulfonates. *J Colloid Interface Sci.* 1983;92(2):561–74. [https://doi.org/10.1016/0021-9797\(83\)90177-7](https://doi.org/10.1016/0021-9797(83)90177-7)
- Belloq AM, Biais J, Clin B, Gelot A, Lalanne P, Lemanceau B. Three-dimensional phase diagram of the brine-toluene-butanol-sodium dodecyl sulfate system. *J Colloid Interface Sci.* 1980;74(2):311–21. [https://doi.org/10.1016/0021-9797\(80\)90200-3](https://doi.org/10.1016/0021-9797(80)90200-3)
- Berti D, Palazzo G. In: Berti D, Palazzo G, editors. *Colloidal foundations of nanoscience.* Amsterdam, Netherlands: Elsevier; 2014.
- Bettenhausen C. Switching to sustainable surfactants. *C&EN.* 2022;100(15):22–7.
- Blochowicz T, Gögelein C, Spehr T, Müller M, Stühn B. Polymer-induced transient networks in water-in-oil microemulsions studied by small-angle x-ray and dynamic light scattering. *Phys Rev E Stat Nonlinear Soft Matter Phys.* 2007;76(4):1505. <https://doi.org/10.1103/PhysRevE.76.041505>
- Borji M, Kharrat A, Ott H. Comparability of in situ crude oil emulsification in phase equilibrium and under porous-media-flow conditions. *J Colloid Interface Sci.* 2022;615:182. <https://doi.org/10.1016/j.jcis.2022.01.182>
- Bourrel M, Salager J-L, Schechter RS, Wade WH. A correlation for phase behavior of nonionic surfactants. *J Colloid Interface Sci.* 1980;75(2):451–61. [https://doi.org/10.1016/0021-9797\(80\)90470-1](https://doi.org/10.1016/0021-9797(80)90470-1)
- Bourrel M, Schechter RS. *Microemulsions and related systems: formulation, solvency, and physical properties.* 2nd ed. Paris, France: Editions Technip; 2010.
- Boyd J, Parkinson C, Sherman P. Factors affecting emulsion stability, and the HLB concept. *J Colloid Interface Sci.* 1972;41(2):359–70. [https://doi.org/10.1016/0021-9797\(72\)90122-1](https://doi.org/10.1016/0021-9797(72)90122-1)
- Cardenas A, Fillous L, Rouviere J, Salager J. An experimental method to estimate the mass transfer through the interfacial region of liquid membrane systems. *Ciencia.* 2001;9(1):70–6.
- Cash R, Cayias JL, Fournier G, McAllister D, Shares T, Schechter RS, et al. The application of low interfacial tension scaling rules to binary hydrocarbon mixtures. *J Colloid Interface*

- Sci. 1977;59(1):39–44. [https://doi.org/10.1016/0021-9797\(77\)90336-8](https://doi.org/10.1016/0021-9797(77)90336-8)
- Cayias JL, Schechter RS, Wade WH. Measurement of low interfacial tension via the spinning drop technique. *ACS Symp Ser.* 1975;8:234–47. <https://doi.org/10.1021/bk-1975-0008.ch017>
- Cayias JL, Schechter RS, Wade WH. Modeling crude oils for low interfacial tension. *Soc Pet Eng J.* 1976;16(6):351–7. <https://doi.org/10.2118/5813-PA>
- Chen SH, Chang SL, Strey R. On the interpretation of scattering peaks from bicontinuous microemulsions. *Progr Colloid Polym Sci.* 1990;81:5519. <https://doi.org/10.1007/bfb0115519>
- Chen SH, Chang SL, Strey R. Simulation of bicontinuous microemulsions. Comparison of simulated real-space microstructures with scattering experiments. *J Appl Crystallogr.* 1991;24(5). <https://doi.org/10.1107/S0021889891001462>
- Choi SM, Chen SH, Sottmann T, Strey R. The existence of three length scales and their relation to the interfacial curvatures in bicontinuous microemulsions. *Physica A.* 2002;304(1–2):85–92. [https://doi.org/10.1016/S0378-4371\(01\)00524-6](https://doi.org/10.1016/S0378-4371(01)00524-6)
- Clausse D, Gomez F, Pezron I, Komunjer L, Dalmazzone C. Morphology characterization of emulsions by differential scanning calorimetry. *Adv Colloid Interf Sci.* 2005;117(1–3):59–74. <https://doi.org/10.1016/j.cis.2005.06.003>
- Croda. *Accelerating our sustainable future – with the ECO range of renewable, bio-based surfactants for personal care.* 2023 <https://www.crodapersonalcare.com/en-gb/our-brands/croda/eco-range>
- Dalmazzone C, Noik C, Clausse D. Application of DSC for emulsified system characterization. *Oil Gas Sci Technol Revue de l'IFP.* 2009;64(5):8041. <https://doi.org/10.2516/ogst:2008041>
- Davies JT. A quantitative kinetic theory of emulsion type. I. Physical chemistry of the emulsifying agent. *Proceedings of the second international congress on surface activity.* Vol 1. London: *Butterworth*; 1957. 426.
- Delforce L, Ontiveros JF, Nardello-Rataj V, Aubry J-M. Rational design of O/W nanoemulsions based on the surfactant dodecylglyceryl ether using the normalized HLD concept and the formulation-composition map. *Colloids Surf A Physicochem Eng Asp.* 2023;167:131679. <https://doi.org/10.1016/j.colsurfa.2023.131679>
- Delgado-Linares JG, Pereira JC, Rondón M, Bullón J, Salager JL. Breaking of water-in-crude oil emulsions. 6. Estimating the demulsifier performance at optimum formulation from both the required dose and the attained instability. *Energy Fuel.* 2016;30(7):5483–91. <https://doi.org/10.1021/acs.energyfuels.6b00666>
- Eastoe J, Yan C, Mohamed A. Microemulsions with CO<sub>2</sub> as a solvent. *Curr Opin Colloid Interface Sci.* 2012;17(5):266–73. <https://doi.org/10.1016/j.cocis.2012.06.006>
- Evonik. *Biosurfactants.* 2021 <https://corporate.evonik.com/misc/micro/biosurfactants/index.en.html>
- Eyssautier J, Frot D, Barré L. Structure and dynamic properties of colloidal asphaltene aggregates. *Langmuir.* 2012;28(33):1707. <https://doi.org/10.1021/la301707h>
- Fillous L, Cardenas A, Rouivere J, Salager J-L. Interfacial mass transfer vs. formulation in multiple phase anionic surfactant-oil-water systems. *J Surfactant Deterg.* 1999;2(3):303–7. <https://doi.org/10.1007/s11743-999-0081-8>
- Fillous L, Cardenas A, Rouvière J, Salager J-L. Interfacial mass transfer versus formulation in multiple phase anionic surfactant-oil-water systems. *J Surfactant Deterg.* 1999;2(3):303–7. <https://doi.org/10.1007/s11743-999-0081-8>
- Forgiarini A, Marquez R, Salager J-L. Formulation improvements in the applications of surfactant-oil-water systems using the HLDN approach with extended surfactant structure. *Molecules.* 2021;26(12):3771. <https://doi.org/10.3390/molecules26123771>
- Fukumoto A, Dalmazzone C, Frot D, Barré L, Noik C. Investigation on physical properties and morphologies of microemulsions formed with sodium dodecyl benzenesulfonate, Isobutanol, brine, and Decane, using several experimental techniques. *Energy Fuel.* 2016;30(6):0595. <https://doi.org/10.1021/acs.energyfuels.6b00595>
- Fukumoto A, Dalmazzone C, Frot D, Barré L, Noik C. Characterization of complex crude oil microemulsions-DSC contribution. *Oil Gas Sci Technol Rev IFP Energies Nouvelles.* 2018;3:73.
- Furó I. NMR spectroscopy of micelles and related systems. *J Mol Liq.* 2005;117(1–3):117–37. <https://doi.org/10.1016/j.molliq.2004.08.010>
- Galindo-Alvarez J, Sadtler V, Choplin L, Salager JL. Viscous oil emulsification by catastrophic phase inversion: influence of oil viscosity and process conditions. *Ind Eng Chem Res.* 2011;50(9):5575–83. <https://doi.org/10.1021/ie102224k>
- Gaur VK, Sharma P, Sirohi R, Varjani S, Taherzadeh MJ, Chang J-S, et al. Production of biosurfactants from agro-industrial waste and waste cooking oil in a circular bioeconomy: an overview. *Bioreour Technol.* 2022;343:126059. <https://doi.org/10.1016/j.biortech.2021.126059>
- Ghosh S, Johns RT. Dimensionless equation of state to predict microemulsion phase behavior. *Langmuir.* 2016;32(35):8969–79. <https://doi.org/10.1021/acs.langmuir.6b02666>
- Graciaa A, Barakat Y, Schechter R, Wade W, Yiv S. Emulsion stability and phase behavior for ethoxylated nonyl phenol surfactants. *J Colloid Interface Sci.* 1982;89(1):217–25. [https://doi.org/10.1016/0021-9797\(82\)90135-7](https://doi.org/10.1016/0021-9797(82)90135-7)
- Graciaa A, Lachaise J, Bourrel M, Osborne-Lee I, Schechter RS, Wade WH. Partitioning of nonionic and anionic surfactant mixtures between oil/microemulsion/water phases. *SPE Reserv Eng.* 1987;2(3):305–14. <https://doi.org/10.2118/13030-pa>
- Gradziński M, Duvail M, de Molina PM, Simon M, Talmon Y, Zemb T. Using microemulsions: formulation based on knowledge of their Mesostucture. *Chem Rev.* 2021;121(10):5671–740. <https://doi.org/10.1021/acs.chemrev.0c00812>
- Griffin W. Classification of surface-active agents by "HLB". *J Soc Cosmet Chem.* 1949;1:311–26.
- Griffin W. Calculation of HLB values of non-ionic surfactants. *J Soc Cosmet Chem.* 1954;5:249.
- Hayes D, Solaiman DK, Ashby RD. *Biobased surfactants: synthesis, properties, and applications.* Amsterdam, The Netherlands: Elsevier; 2019. <https://doi.org/10.1016/C2016-0-03179-0>
- Hellweg T. *Scattering techniques to study the microstructure of microemulsions: background, new concepts, applications, perspectives.* Hoboken, NJ: Wiley; 2009. <https://doi.org/10.1002/9781444305524.ch2>
- Herrera D, Chevalier T, Fleury M, Dalmazzone C. Quantification of microemulsion systems using low-field T1-weighted imaging. *Magn Reson Imaging.* 2021;83:160–8. <https://doi.org/10.1016/j.mri.2021.08.002>
- Herrera D, Chevalier T, Frot D, Barré L, Drelich A, Pezron I, et al. Monitoring the formation kinetics of a bicontinuous microemulsion. *J Colloid Interface Sci.* 2022;609:200–11. <https://doi.org/10.1016/j.jcis.2021.12.011>
- Huh C. Interfacial tensions and solubilizing ability of a microemulsion phase that coexists with oil and brine. *J Colloid Interface Sci.* 1979;71(2):408–26. [https://doi.org/10.1016/0021-9797\(79\)90249-2](https://doi.org/10.1016/0021-9797(79)90249-2)
- Hyde S, Andersson S, Larsson K, Landh T, Blum Z, Ninham B. In: Hyde S, Andersson S, Larsson K, Landh T, Blum Z, Ninham B, editors. *The language of shape: the role of curvature in condensed matter: physics, chemistry and biology.* Amsterdam, The Netherlands: Elsevier Science B.V.; 1997. <https://doi.org/10.1016/B978-044481538-5/50002-2>
- Israelachvili JN, Mitchell DJ, Ninham BW. Theory of self assembly of hydrocarbon amphiphiles into micelles and bilayers. *J Chem Soc, Faraday Trans 2.* 1976;72:1525. <https://doi.org/10.1039/f29767201525>
- Johnson GK, Dadyburjor DB, Smith DH. Electrical conductivities of three-phase emulsions. 2. C<sub>6</sub>H<sub>13</sub> (OC<sub>2</sub>H<sub>4</sub>)<sub>2</sub>OH/n-

- tetradecane/water with wetting and nonwetting middle phases. *Langmuir*. 1994;10(8):2523–7. <https://doi.org/10.1021/la00020a007>
- Jouffroy J, Levinson P, de Gennes PG. Phase equilibria involving microemulsions (remarks on the Talmon-Prager model). *J Phys (Paris)*. 1982;43(8):1241–8. <https://doi.org/10.1051/jphys:019820043080124100>
- Kabalnov A, Wennerström H. Macroemulsion stability: the oriented wedge theory revisited. *Langmuir*. 1996;12(2):276–92. <https://doi.org/10.1021/la950359e>
- Kashif A, Rehman R, Fuwad A, Shahid MK, Dayarathne HNP, Jamal A, et al. Current advances in the classification, production, properties and applications of microbial biosurfactants – a critical review. *Adv Colloid Interf Sci*. 2022;306:102718. <https://doi.org/10.1016/j.cis.2022.102718>
- Kim YH, Wasan DT. Effect of Demulsifier partitioning on the destabilization of water-in-oil emulsions. *Ind Eng Chem Res*. 1996;35(4):1141. <https://doi.org/10.1021/ie950372u>
- Kiran SK, Acosta E. HLD–NAC and the formation and stability of emulsions near the phase inversion point. *Ind Eng Chem Res*. 2015;54(25):6467–79. <https://doi.org/10.1021/acs.iecr.5b00382>
- Klaus EE, Jones JH, Nagarajan R, Ertekin T, Chung YM, Arf G, et al. Generation of ultralow tensions over a wide EACN range using Pennsylvania state U. Surfactants. *Soc Pet Eng J*. 1983;23(1):73–80. <https://doi.org/10.2118/9784-PA>
- Kunz W, Holmberg K, Zemb T. Hydrotropes. *Curr Opin Colloid Interface Sci*. 2016;22:99–107. <https://doi.org/10.1016/j.cocis.2016.03.005>
- Kunz W, Testard F, Zemb T. Correspondence between curvature, packing parameter, and hydrophilic-lipophilic deviation scales around the phase-inversion temperature. *Langmuir*. 2009;25(1):112–5. <https://doi.org/10.1021/la8028879>
- Kunz W, Zemb T, Harrar A. Using ionic liquids to formulate microemulsions: current state of affairs. *Curr Opin Colloid Interface Sci*. 2012;17(4):205–11. <https://doi.org/10.1016/j.cocis.2012.03.002>
- Langevin D. Emulsions, microemulsions and foams. Berlin, Germany: Springer; 2020. <https://doi.org/10.1007/978-3-030-55681-5>
- Lee JM, Lim KH. Changes in two-phase emulsion morphology in temperature–amphiphile concentration or fish diagram for ternary amphiphile/oil/water systems. *J Colloid Interface Sci*. 2005;290:241.
- Lee JM, Shin HJ, Lim KH. Morphologies of three-phase emulsions of the ternary nonionic amphiphile/oil/water systems and their determination by electrical method. *J Colloid Interface Sci*. 2003;257(2):344–56. [https://doi.org/10.1016/S0021-9797\(02\)00051-6](https://doi.org/10.1016/S0021-9797(02)00051-6)
- Lemahieu G, Ontiveros JF, Gaudin T, Molinier V, Aubry JM. The salinity-phase-inversion method (SPI-slope): a straightforward experimental approach to assess the hydrophilic-lipophilic-ratio and the salt-sensitivity of surfactants. *J Colloid Interface Sci*. 2022;608:549–63. <https://doi.org/10.1016/j.cis.2021.09.155>
- Lemahieu G, Ontiveros JF, Terra N, Souza T, Aubry J-M, Terra Telles Souza N, et al. Fast and accurate selection of surfactants for enhanced oil recovery by dynamic salinity-phase-inversion (SPI). *Fuel*. 2021;289(2020):119928. <https://doi.org/10.1016/j.fuel.2020.119928>
- Lemyre JL, Lamarre S, Beaupré A, Ritcey AM. A new approach for the characterization of reverse micellar systems by dynamic light scattering. *Langmuir*. 2010;26(13):541. <https://doi.org/10.1021/la100541m>
- Leng Z, Acosta E. The characteristic curvature (CC) definition and its use in assessing CC for single ionic surfactants. *J Surfactant Deterg*. 2023;26(3):287–301. <https://doi.org/10.1002/jsde.12653>
- Lif A, Nydén M, Holmberg K. Water-in-diesel microemulsions studied by NMR diffusometry. *J Dispers Sci Technol*. 2009;30(6):4079. <https://doi.org/10.1080/01932690802644079>
- Lindman B, Kamenka N, Kathopoulis TM, Brun B, Nilsson PG. Translational diffusion and solution structure of microemulsions. *J Phys Chem*. 1980;84(19):027. <https://doi.org/10.1021/j100456a027>
- Lindman B, Olsson U, Soderman O. Characterization of microemulsions by NMR. *Handbook of microemulsion science and technology*. Boca Raton: CRC Press; 2020. <https://doi.org/10.1201/9780203752739-10>
- Marfisi S, Rodríguez MP, Alvarez G, Celis M-T, Forgiarini A, Lachaise J, Salager JL. Complex emulsion inversion pattern associated with the partitioning of nonionic surfactant mixtures in the presence of alcohol cosurfactant. *Langmuir*. 2005;21:6712. <https://doi.org/10.1021/la050450a>
- Marquez L, Graciaa A, Lachaise J, Salager J-L, Zambrano N. Hysteresis behaviour in temperature-induced emulsion inversion. *Polym Int*. 2003;52(4):590–3. <https://doi.org/10.1002/pi.1046>
- Marquez N, Anton RE, Graciaa A, Lachaise J, Salager JL. Partitioning of ethoxylated alkylphenol surfactants in microemulsion-oil-water systems. *Colloids Surf A Physicochem Eng Asp*. 1995;100:225–31. [https://doi.org/10.1016/0927-7757\(95\)03184-F](https://doi.org/10.1016/0927-7757(95)03184-F)
- Márquez N, Anton RE, Graciaa A, Lachaise J, Salager J-L. Partitioning of ethoxylated alkylphenol surfactants in microemulsion-oil-water systems. Part II: influence of hydrophobe branching. *Colloids Surf A Physicochem Eng Asp*. 1998;131(1–3):45–9. [https://doi.org/10.1016/S0927-7757\(96\)03944-1](https://doi.org/10.1016/S0927-7757(96)03944-1)
- Marquez R, Acevedo N, Rondón M, Graciaa A, Daridon J-L, Salager J-L. Breaking of water-in-crude oil emulsions. 10. Experimental evidence from a quartz crystal resonator sensor and an oscillating spinning drop interfacial rheometer. *Energy Fuel*. 2023;37:2735–49. <https://doi.org/10.1021/acs.energyfuels.2c03717>
- Marquez R, Antón RE, Vejar F, Salager J-L, Forgiarini AM. New interfacial rheology characteristics measured using a spinning drop rheometer at the optimum formulation. Part 2. Surfactant–oil–water systems with a high volume of middle-phase microemulsion. *J Surfactant Deterg*. 2019;22(2):177–88. <https://doi.org/10.1002/jsde.12245>
- Marquez R, Bullon J, Forgiarini A, Salager J-L. The oscillatory spinning drop technique. An innovative method to measure dilational interfacial rheological properties of brine-crude oil systems in the presence of asphaltenes. *Colloids Interfaces*. 2021;5(3):42. <https://doi.org/10.3390/colloids5030042>
- Marquez R, Forgiarini AM, Fernández J, Langevin D, Salager J-L. New interfacial rheology characteristics measured using a spinning-drop rheometer at the optimum formulation of a simple surfactant–oil–water system. *J Surfactant Deterg*. 2018;21(5):611–23. <https://doi.org/10.1002/jsde.12163>
- Marquez R, Forgiarini AM, Langevin D, Salager J-L. Instability of emulsions made with surfactant–oil–water systems at optimum formulation with ultralow interfacial tension. *Langmuir*. 2018;34(31):9252–63. <https://doi.org/10.1021/acs.langmuir.8b01376>
- Marquez R, Forgiarini AM, Langevin D, Salager J-L. Breaking of water-in-crude oil emulsions. Part 9. New interfacial rheology characteristics measured using a spinning drop rheometer at optimum formulation. *Energy Fuel*. 2019;33(9):8151–64. <https://doi.org/10.1021/acs.energyfuels.9b01476>
- Marquez R, Meza L, Alvarado J, Johnny B, Langevin D, Forgiarini A, et al. Interfacial rheology measured with a spinning drop interfacial rheometer: more realistic surfactant-oil-water systems close to optimum formulation at HLDN=0. *J Surfactant Deterg*. 2021. <https://doi.org/10.1002/jsde.12502>
- Marquez R, Meza L, Alvarado JG, Bullón J, Langevin D, Forgiarini AM, et al. Interfacial rheology measured with a spinning drop interfacial rheometer: particularities in more realistic surfactant–oil–water systems close to optimum formulation at HLDN = 0. *J Surfactant Deterg*. 2021;24(4):587–601. <https://doi.org/10.1002/jsde.12502>
- Maru HC, Wasan DT. Dilational viscoelastic properties of fluid interfaces-II. *Chem Eng Sci*. 1979;34(11):1295. [https://doi.org/10.1016/0009-2509\(79\)80021-4](https://doi.org/10.1016/0009-2509(79)80021-4)
- McClements DJ. Critical review of techniques and methodologies for characterization of emulsion stability. *Crit Rev Food Sci Nutr*. 2007;47(7):611–49. <https://doi.org/10.1080/10408390701289292>

- Miller CA, Hwan R-N, Benton WJ, Fort T Jr. Ultralow interfacial tensions and their relation to phase separation in micellar solutions. *J Colloid Interface Sci.* 1977;61(3):554–68. [https://doi.org/10.1016/0021-9797\(77\)90473-8](https://doi.org/10.1016/0021-9797(77)90473-8)
- Milos FS, Wasan DT. Emulsion stability of surfactant systems near the three phase region. *Colloids Surf.* 1982;4(1):91–6. [https://doi.org/10.1016/0166-6622\(82\)80092-9](https://doi.org/10.1016/0166-6622(82)80092-9)
- Miñana-Pérez M, Gutron MC, Zundel C, Andérez J, Salager J-L. Mini-emulsion formation by transitional inversion. *J Dispers Sci Technol.* 1999;20:893. <https://doi.org/10.1080/01932699908943826>
- Miñana-Pérez M, Jarry P, Pérez-Sánchez M, Ramirez-Gouveia M, Salager J-L. Surfactant-oil-water systems near the affinity inversion part V: properties of emulsions. *J Dispers Sci Technol.* 1986;7(3):331–43. <https://doi.org/10.1080/01932698608943464>
- Nagarajan R. Molecular packing parameter and surfactant self-assembly: the neglected role of the surfactant tail. *Langmuir.* 2002;18(1):31–8. <https://doi.org/10.1021/la010831y>
- Nguyen TT, Sabatini DA. Formulating alcohol-free microemulsions using rhamnolipid biosurfactant and rhamnolipid mixtures. *J Surfactant Deterg.* 2009;12(2):109–15. <https://doi.org/10.1007/s11743-008-1098-y>
- Nguyen TT, Sabatini DA. Characterization and emulsification properties of rhamnolipid and sophorolipid biosurfactants and their applications. *Int J Mol Sci.* 2011;12(2):1232–44. <https://doi.org/10.3390/ijms12021232>
- Ontiveros JF, Pierlot C, Catté M, Molinier V, Pizzino A, Salager J-L, et al. Classification of ester oils according to their equivalent alkane carbon number (EACN) and asymmetry of fish diagrams of C10E4/ester oil/water systems. *J Colloid Interface Sci.* 2013;403:67–76. <https://doi.org/10.1016/j.jcis.2013.03.071>
- Ontiveros JF, Pierlot C, Catté M, Salager JL, Aubry JM. Determining the preferred alkane carbon number (PACN) of nonionic surfactants using the PIT-slope method. *Colloids Surf A Physicochem Eng Asp.* 2018;536(2016):30–7. <https://doi.org/10.1016/j.colsurfa.2017.08.002>
- Ortiz M, Alvarado JG, Zambrano F, Marqu-ez R. Surfactants produced from carbohydrate derivatives. A review of the biobased building blocks used in their synthesis. *J Surfactant Deterg.* 2022. <https://doi.org/10.1002/jsde.12581>
- Pierlot C, Menuge M, Catté M, Devos O, Ontiveros JF. Visible light backscattering monitored in situ for transitional phase inversion of BrijL4-isopropyl myristate-water emulsions. *Ind Eng Chem Res.* 2019;58(44):20195–202. <https://doi.org/10.1021/acs.iecr.9b04062>
- Pierlot C, Ontiveros JF, Catté M, Salager J-L, Aubry JM. Cone-plate rheometer as reactor and viscosity probe for the detection of transitional phase inversion of Brij30-isopropyl myristate-water model emulsion. *Ind Eng Chem Res.* 2016;55(14):3990–9. <https://doi.org/10.1021/acs.iecr.6b00399>
- Pizzino A, Molinier V, Catté M, Ontiveros JF, Salager J-L, Aubry J-M. Relationship between phase behavior and emulsion inversion for a well-defined surfactant (C10E4)/ n-octane/water ternary system at different temperatures and water/oil ratios. *Ind Eng Chem Res.* 2013;52(12):4527–38. <https://doi.org/10.1021/ie302772u>
- Pizzino A, Rodriguez MP, Xuereb C, Catté M, Van Hecke E, Aubry JM, et al. Light backscattering as an indirect method for detecting emulsion inversion. *Langmuir.* 2007;23(10):5286–8. <https://doi.org/10.1021/la070090m>
- Pouchelon A, Chatenay D, Meunier J, Langevin D. Origin of low interfacial tensions in systems involving microemulsion phases. *J Colloid Interface Sci.* 1981;82(2):418–22. [https://doi.org/10.1016/0021-9797\(81\)90383-0](https://doi.org/10.1016/0021-9797(81)90383-0)
- Pouchelon A, Meunier J, Langevin D, Chatenay D, Cazabat AM. Low interfacial tensions in three-phase systems obtained with oil-water surfactant mixtures. *Chem Phys Lett.* 1980;76(2):277–81. [https://doi.org/10.1016/0009-2614\(80\)87020-5](https://doi.org/10.1016/0009-2614(80)87020-5)
- Prévost S, Gradzielski M, Zemb T. Self-assembly, phase behaviour and structural behaviour as observed by scattering for classical and non-classical microemulsions. *Adv Colloid Interf Sci.* 2017;247:374–96. <https://doi.org/10.1016/j.cis.2017.07.022>
- Prince L. Schulman's Microemulsions. In: Prince L, editor. *Microemulsions theory and practice.* New York: Academic Press; 1977. p. 1–20. <https://doi.org/10.1016/B978-0-12-565750-1.50006-0>
- Puerto MC, Gale WW. Estimation of optimal salinity and solubilisation parameters for alkyl Orthoxylene sulfonate mixtures. *Soc Pet Eng J.* 1977;17:193. <https://doi.org/10.2118/5814-PA>
- Queste S, Salager JL, Strey R, Aubry JM. The EACN scale for oil classification revisited thanks to fish diagrams. *J Colloid Interface Sci.* 2007;312(1):98–107. <https://doi.org/10.1016/j.jcis.2006.07.004>
- Rámirez M, Bullón J, Andérez J, Mira I, Salager JL. Drop size distribution bimodality and its effect on O/W emulsion viscosity. *J Dispers Sci Technol.* 2002;23(1–3):309–21. <https://doi.org/10.1081/DIS-120003322>
- Reed RL, Healy RN. Some physicochemical aspects of microemulsion flooding: a review. In: Shah DO, Schecter RS, editors. *Improved oil recovery by surfactant and polymer flooding.* Amsterdam, The Netherlands: Academic Press; 1977. p. 383–437.
- Reger M, Sekine T, Hoffmann H. Boosting the stability of protein emulsions by the synergistic use of proteins and clays. *Colloid Polym Sci.* 2012;290(7):631–40. <https://doi.org/10.1007/s00396-011-2578-6>
- Rondón-González M, Sadtler V, Choplin L, Salager J-L. Emulsion catastrophic inversion from abnormal to normal morphology. 5. Effect of the water-to-oil ratio and surfactant concentration on the inversion produced by continuous stirring. *Ind Eng Chem Res.* 2006;45(9):3074–80. <https://doi.org/10.1021/ie060036l>
- Rosen MJ, Dahanayake M. *Industrial utilization of surfactants: principles and practice.* Urbana, IL: AOCS Press; 2000.
- Roshan Deen G, Pedersen JS. Phase behavior and microstructure of C12e5 nonionic microemulsions with chlorinated oils. *Langmuir.* 2008;24(7):323. <https://doi.org/10.1021/la703323n>
- Rout D, Goyal R, Sinha R, Nagarajan A, Paul P. Predictive modeling of microemulsion phase behaviour and microstructure characterisation in the 1-phase region. *Microemulsions.* 2012;83–94. Chapter 4. <https://doi.org/10.5772/35539>
- Ruckenstein E. Microemulsions, macroemulsions, and the Bancroft rule. *Langmuir.* 1996;12(26):6351. <https://doi.org/10.1021/la960849m>
- Salager J-L. *Physico-chemical properties of surfactant-water-oil mixtures: phase behavior, micro-emulsion formation and interfacial tension.* University of Texas at Austin, Ph.D. Dissertation. 1977.
- Salager J-L. Phase behavior of amphiphile–oil–water systems related to the butterfly catastrophe. *J Colloid Interface Sci.* 1985;105(1):21–6. [https://doi.org/10.1016/0021-9797\(85\)90342-X](https://doi.org/10.1016/0021-9797(85)90342-X)
- Salager J-L. Phase transformation and emulsion inversion on the basis of catastrophe theory. In: Becker P, editor. *Encyclopedia of emulsion technology.* Vol. 3. Basic theory, measurement, applications (vol. 3, pp. 79–134). New York City: Marcell Dekker, Inc.; 1988.
- Salager J-L. Quantifying the concept of physico-chemical formulation in surfactant-oil-water systems—state of the art. *Progr Colloid Polym Sci.* 1996;100:137–42. <https://doi.org/10.1007/bfb0115768>
- Salager J-L. Emulsion properties and related know-how to attain them. In: Nielloud F, Marti-Mestres G, editors. *Pharmaceutical emulsions and suspensions.* Volume 1. New York City: Marcel Dekker; 2000. p. 73–125. <https://doi.org/10.1201/b14005>
- Salager J-L. Surfactants in aqueous solution. Vol E201. Merida, Venezuela: FIRP Booklet; 2002. <https://es.firp-ula.org/wp-content/uploads/2019/07/E201A.pdf>
- Salager J-L. Emulsion phase inversion phenomena. In: Sjoblom J, editor. *Emulsions and emulsion stability.* Boca Raton, FL: CRC Publishing; 2006. p. 185.
- Salager J-L. A normalized hydrophilic-lipophilic deviation expression HLDN is necessary to avoid confusions close to the optimum



- formulation of surfactant-oil-water systems. *J Surfactant Deterg.* 2021;24(5):731–48. <https://doi.org/10.1002/jsde.12518>
- Salager J-L, Antón RE, Arandia MA, Forgiarini AM. How to attain ultralow interfacial tension and three-phase behavior with surfactant formulation for enhanced oil recovery: a review. Part 4: robustness of the optimum formulation zone through the insensitivity to some variables and the occurrence of complex artifacts. *J Surfactant Deterg.* 2017;20(5):987–1018. <https://doi.org/10.1007/s11743-017-2000-6>
- Salager J-L, Antón RE, Bullón J, Forgiarini A, Marquez R. How to use the normalized hydrophilic-lipophilic deviation (HLDN) concept for the formulation of equilibrated and emulsified surfactant-oil-water systems for cosmetics and pharmaceutical products. *Cosmetics.* 2020;7(3):57. <https://doi.org/10.3390/cosmetics7030057>
- Salager J-L, Bourrel M, Schechter RS, Wade WH. Mixing rules for optimum phase behavior formulation of surfactant-oil-water systems. *Soc Pet Eng J.* 1979;19(5):271–8. <https://doi.org/10.2118/7584-pa>
- Salager J-L, Bullón J, Pizzino A, Rondón-González M, Tolosa L. Emulsion formulation engineering for the practitioner. In: Somasundaran P, editor. *Encyclopedia of surface and colloid science.* Volume 1. 3rd. ed. New York: Taylor & Francis; 2010. p. 1–6. <https://doi.org/10.1081/E-ESCS-120045970>
- Salager J-L, Forgiarini A, Marquez L, Peña A. Inversion d'émulsion dans la mise en oeuvre de procédés industriels emulsion inversion as a tool in industrial processes. Lyon, France: World Congress on Emulsion; 2002.
- Salager J-L, Forgiarini A, Marquez R. Extended surfactants including an alkoxylated central part intermediate producing a gradual polarity transition—a review of the properties used in applications such as enhanced oil recovery and polar oil solubilization in microemulsions. *J Surfactant Deterg.* 2019;22(5):935–72. <https://doi.org/10.1002/jsde.12331>
- Salager J-L, Forgiarini AM, Bullón J. How to attain ultralow interfacial tension and three-phase behavior with surfactant formulation for enhanced oil recovery: a review. Part 1. Optimum formulation for simple surfactant-oil-water ternary systems. *J Surfactant Deterg.* 2013;16(4):449–72. <https://doi.org/10.1007/s11743-013-1470-4>
- Salager J-L, Forgiarini AM, Márquez L, Manchego L, Bullón J, Marquez L, et al. How to attain an ultralow interfacial tension and a three-phase behavior with a surfactant formulation for enhanced oil recovery: a review. Part 2. Performance improvement trends from Winsor's premise to currently proposed inter- and intra-molecular mixtu. *J Surfactant Deterg.* 2013;16(5):631–63. <https://doi.org/10.1007/s11743-013-1485-x>
- Salager J-L, Graciaa A, Marquez R. Analyzing the surfactant classification confusion through the HLD formulation equation. *JCS Open.* 2022;8:100060. <https://doi.org/10.1016/j.jciso.2022.100060>
- Salager J-L, Loaiza-Maldonado I, Miñana-Perez M, Silva F. Surfactant-oil-water systems near the affinity inversion part I: relationship between equilibrium phase behavior and emulsion type and stability. *J Dispers Sci Technol.* 1982;3(3):279–92. <https://doi.org/10.1080/01932698208943642>
- Salager J-L, Lopez-Castellanos G, Miñana-Perez M. Surfactant-oil-water systems near the affinity inversion: part VI: emulsions with viscous hydrocarbons. *J Dispers Sci Technol.* 1990;11(4):397–407. <https://doi.org/10.1080/01932699008943262>
- Salager J-L, Márquez L, Peña AA, Rondón M, Silva F, Tyrode E. Current phenomenological know-how and modeling of emulsion inversion. *Ind Eng Chem Res.* 2000;39(8):2665–76. <https://doi.org/10.1021/ie990778x>
- Salager JL, Márquez N, Antón RE, Graciaa A, Lachaise J. Retrograde transition in the phase behavior of surfactant–oil–water systems produced by an alcohol scan. *Langmuir.* 1995;11(1):37–41. <https://doi.org/10.1021/la00001a010>
- Salager J-L, Marquez N, Graciaa A, Lachaise J. Partitioning of ethoxylated octylphenol surfactants in microemulsion-oil-water systems: influence of temperature and relation between partitioning coefficient and physicochemical formulation. *Langmuir.* 2000;16(13):5534–9. <https://doi.org/10.1021/la9905517>
- Salager J-L, Marquez R, Bullon J, Forgiarini A. Formulation in surfactant systems: from-Winsor-to-HLDN. *Encyclopedia.* 2022;2(2):054. <https://doi.org/10.3390/encyclopedia2020054>
- Salager J-L, Marquez R, Delgado-Linares JG, Rondon M, Forgiarini A. Fundamental basis for action of a chemical demulsifier revisited after 30 years: HLDN as the primary criterion for water-in-crude oil emulsion breaking. *Energy Fuel.* 2022;36(2):711–30. <https://doi.org/10.1021/acs.energyfuels.1c03349>
- Salager J-L, Marquez R, Ontiveros JF. How to use in practice a simplified HLDN linear equation for surfactant mixtures. *Proceedings of the 2022 AOCs annual meeting.* 2022.
- Salager J-L, Marquez R, Rondón M, Bullón J, Graciaa A. Review on some confusion produced by the bicontinuous microemulsion terminology and its domains microcurvature: a simple spatiotemporal model at optimum formulation of surfactant-oil-water systems. *ACS Omega.* 2023;10:9040–57. <https://doi.org/10.1021/acsomega.3c00547>
- Salager J-L, MiñanaPerez M, Anderez JM, Grosso JL, Rojas CI, Layrisse I. Surfactant-oil-water systems near the affinity inversion part II: viscosity of emulsified systems. *J Dispers Sci Technol.* 1983;4(2):161–73. <https://doi.org/10.1080/01932698308943361>
- Salager J-L, Miñana-Pérez M, Pérez-Sánchez M, Ramirez-Gouveia M, Rojas CI. Surfactant-oil-water systems near the affinity inversion part III: the two kinds of emulsion inversion. *J Dispers Sci Technol.* 1983;4(3):313. <https://doi.org/10.1080/01932698308943373>
- Salager J-L, Moreno N, Antón RE, Marfisi S. Apparent equilibration time required for a surfactant-oil-water system to emulsify into the morphology imposed by the formulation. *Langmuir.* 2002;18(3):607–11. <https://doi.org/10.1021/la010582d>
- Salager J-L, Morgan JC, Schechter RS, Wade WH, Vasquez E. Optimum formulation of surfactant/water/oil systems for minimum interfacial tension or phase behavior. *Soc Pet Eng J.* 1979;19(2):107–15. <https://doi.org/10.2118/7054-PA>
- Schirone D, Gentile L, Olsson U, Palazzo G. Optimum formulation conditions for cationic surfactants via rheo-titration in turbulent regime. *Colloids Surf A Physicochem Eng Asp.* 2022;648:129154. <https://doi.org/10.1016/j.colsurfa.2022.129154>
- Schubert KV, Strey R, Kahlweit M. Similarities of aqueous and nonaqueous microemulsions. *Progr Colloid Polym Sci.* 1992;89:263–7. <https://doi.org/10.1007/bfb0116325>
- Schulman JH, Stoeckenius W, Prince LM. Mechanism of formation and structure of micro emulsions by electron microscopy. *J Phys Chem.* 1959;63(10):1677–80. <https://doi.org/10.1021/j150580a027>
- Scriven LE. Equilibrium bicontinuous structure. *Nature.* 1976;263(5573):123–5. <https://doi.org/10.1038/263123a0>
- Scriven LE. Equilibrium bicontinuous structures. In: Mittal KL, editor. *Micellization, solubilization, and microemulsions.* Berlin, Germany: Springer; 1977. p. 877–93. [https://doi.org/10.1007/978-1-4613-4157-4\\_23](https://doi.org/10.1007/978-1-4613-4157-4_23)
- Shah DO, Schechter RS. Improved oil recovery by surfactant and polymer flooding. Amsterdam, The Netherlands: Elsevier; 1977. <https://doi.org/10.1016/B978-0-126-41750-0.X5001-4>
- Shinoda K. The correlation between the dissolution state of nonionic surfactant and the type of dispersion stabilized with the surfactant. *J Colloid Interface Sci.* 1967;24(1):4. [https://doi.org/10.1016/0021-9797\(67\)90270-6](https://doi.org/10.1016/0021-9797(67)90270-6)
- Shinoda K, Sagitani H. Emulsifier selection in water/oil type emulsions by hydrophile–lipophile balance–temperature system. *J Colloid Interface Sci.* 1978;64:68. [https://doi.org/10.1016/0021-9797\(78\)90335-1](https://doi.org/10.1016/0021-9797(78)90335-1)
- Shinoda K, Saito H. The stability of O/W type emulsions as functions of temperature and the HLB of emulsifiers: the emulsification by

- PIT-method. *J Colloid Interface Sci.* 1969;30(2):258–63. [https://doi.org/10.1016/S0021-9797\(69\)80012-3](https://doi.org/10.1016/S0021-9797(69)80012-3)
- Shukla A, Graener H, Neubert RHH. Observation of two diffusive relaxation modes in microemulsions by dynamic light scattering. *Langmuir.* 2004;20(20):8526–30. <https://doi.org/10.1021/la048883l>
- Silva F, Peña A, Miñana-Pérez M, Salager J-L. Dynamic inversion hysteresis of emulsions containing anionic surfactants. *Colloids Surf A.* 1998;132:221. [https://doi.org/10.1016/s0927-7757\(97\)00208-2](https://doi.org/10.1016/s0927-7757(97)00208-2)
- Silva EJ, Zaniquelli MED, Loh W. Light-scattering investigation on microemulsion formation in mixtures of diesel oil (or hydrocarbons)+ ethanol+ additives. *Energy Fuel.* 2007;21(1):222–6. <https://doi.org/10.1021/ef060264s>
- Slattery JC, den Chen J, Thomas CP, Fleming PD. Spinning drop interfacial viscometer. *J Colloid Interface Sci.* 1980;73(2):483–99. [https://doi.org/10.1016/0021-9797\(80\)90095-8](https://doi.org/10.1016/0021-9797(80)90095-8)
- Smith DH, Johnson GK, Wang Y-HC, Lim K-H. Electrical conductivities of three-phase emulsions. 1. Strongly wetting middle phase. *Langmuir.* 1994;10(8):2516–22. <https://doi.org/10.1021/la00020a006>
- Smith DH, Lim K-H. History and status of the emulsion morphology diagram for two- and three-phase emulsions. *J Ind Eng Chem.* 2000;6(4):201–11.
- Sottmann T, Strey R. Ultralow interfacial tensions in water–n-alkane–surfactant systems. *J Chem Phys.* 1997;106(20):8606–15. <https://doi.org/10.1063/1.473916>
- Tadros TF. *Applied surfactants: principles and applications.* Hoboken, NJ: John Wiley & Sons; 2006.
- Tambe D, Paulis J, Sharma MM. Factors controlling the stability of colloid-stabilized emulsions. *J Colloid Interface Sci.* 1995;171:463. <https://doi.org/10.1006/jcis.1993.1182>
- Tambe DE, Sharma MM. Hydrodynamics of thin liquid films bounded by viscoelastic interfaces. *J Colloid Interface Sci.* 1991;147(1):137–51. [https://doi.org/10.1016/0021-9797\(91\)90142-U](https://doi.org/10.1016/0021-9797(91)90142-U)
- Tartaro G, Gentile L, Palazzo G. Characteristic length and curvature of the AOT/brine/squalane “sponge” L3 phases. *JCIS Open.* 2023;9:100077. <https://doi.org/10.1016/j.jciso.2023.100077>
- Teubner M, Strey R. Origin of the scattering peak in microemulsions. *J Chem Phys.* 1987;87(5):3006. <https://doi.org/10.1063/1.453006>
- Tolosa LI, Forgiarini A, Moreno P, Salager J-L. Combined effects of formulation and stirring on emulsion drop size in the vicinity of three-phase behavior of surfactant-oil water systems. *Ind Eng Chem Res.* 2006;45(11):3810–4. <https://doi.org/10.1021/ie060102j>
- Unsal E, Rücker M, Berg S, Bartels WB, Bonnin A. Imaging of compositional gradients during in situ emulsification using X-ray micro-tomography. *J Colloid Interface Sci.* 2019;550:068. <https://doi.org/10.1016/j.jcis.2019.04.068>
- van Blaaderen A, Vrij A. Synthesis and characterization of colloidal dispersions of fluorescent, monodisperse silica spheres. *Langmuir.* 1992;8(12):2921–31. <https://doi.org/10.1021/la00048a013>
- Vera R, Salazar-Rodríguez F, Marquez R, Forgiarini AM. How the influence of different salts on interfacial properties of surfactant–oil–water systems at optimum formulation matches the Hofmeister series ranking. *J Surfactant Deterg.* 2020;23(3):603–15. <https://doi.org/10.1002/jsde.12406>
- Vinatieri JE. Correlation of emulsion stability with phase behavior in surfactant systems for tertiary oil recovery. *Soc Pet Eng J.* 1980;20(5):402–6. <https://doi.org/10.2118/6675-PA>
- Vitale SA, Katz JL. Liquid droplet dispersions formed by homogeneous liquid-liquid nucleation: “the ouzo effect”. *Langmuir.* 2003;19(10):4105–10. <https://doi.org/10.1021/la026842o>
- Wade W, Morgan JC, Schechter RS, Jacobson JK, Salager J-L. Interfacial tension and phase behavior of surfactant systems. *Soc Pet Eng J.* 1978;18(4):242–52. <https://doi.org/10.2118/6844-PA>
- Wasan DT, McNamara JJ, Shah SM, Sampath K, Aderangi N. The role of coalescence phenomena and interfacial rheological properties in enhanced oil recovery: an overview. *J Rheol.* 1979;23(2):181–207. <https://doi.org/10.1122/1.549524>
- Wasan DT, Mohan V. Interfacial rheological properties of fluid interfaces containing surfactants. In: Shah D, Schechter RS, editors. *Improved oil recovery by surfactant and polymer flooding.* New York City: Academic Press, Inc; 1977. p. 161–203. <https://doi.org/10.1016/b978-0-12-641750-0.50011-6>
- Winsor P. Hydrotrophy, solubilisation and related emulsification processes. *Trans Faraday Soc.* 1948;44:376–98. <https://doi.org/10.1039/TF9484400376>
- Winsor P. *Solvent properties of amphiphilic compounds.* London, UK: Butterworths Scientific Publications; 1954.
- Winsor PA. Binary and multicomponent solutions of amphiphilic compounds. Solubilization and the formation, structure, and theoretical significance of liquid crystalline solutions. *Chem Rev.* 1968;68(1):1–40. <https://doi.org/10.1021/cr60251a001>
- Zamora JM, Marquez R, Forgiarini A, Langevin D, Salager J-L. Interfacial rheology of low interfacial tension systems using a new oscillating spinning drop method. *J Colloid Interface Sci.* 2018;519:27–37. <https://doi.org/10.1016/j.jcis.2018.02.015>
- Zemb TN, Klossek M, Lopian T, Marcus J, Schöettl S, Horinek D, et al. How to explain microemulsions formed by solvent mixtures without conventional surfactants. *Proc Natl Acad Sci.* 2016;113(16):4260–5. <https://doi.org/10.1073/pnas.1515708113>

**How to cite this article:** Marquez R, Ontiveros JF, Barrios N, Tolosa L, Palazzo G, Nardello-Rataj V, et al. Advantages and limitations of different methods to determine the optimum formulation in surfactant–oil–water systems: A review. *J Surfact Deterg.* 2023. <https://doi.org/10.1002/jsde.12703>